A priori error analysis of shape derivatives of linear functionals in structural topology optimization

Aaron Klein[a], Prasanth B. Nair[a], Masayuki Yano[a,*]

[a] *University of Toronto Institute for Aerospace Studies, 4925 Dufferin St, Toronto, M3H 5T6, Canada*

Abstract

We provide theoretical analyses and numerical comparisons of boundary-based and volumetric shape derivative expressions of linear objective functionals encountered in topology optimization of linear elastic structures. The two expressions yield identical results if the domain is smooth and the governing equation is solved exactly; however, the finite element approximation of the expressions for less regular domains yield different results. We first review the two expressions to show that the volumetric shape derivative places weaker regularity requirements, which, unlike the requirements for boundary-based shape derivatives, are satisfied in most finite element approximations. We then analyze the error in the degree-k polynomial finite element approximations of the two expressions; we show that, for sufficiently regular problems, the boundary-based and volumetric shape derivatives provide k-th and $2k$-th order accurate approximations, respectively, of the true shape derivative. We finally assess, through numerical examples, the practical implications of using the volumetric vs boundary-based shape derivatives in topology optimization problems; we demonstrate that methods based on the volumetric shape derivative yield more robust solutions to topology optimization problems.

1. Introduction

Topology optimization has been an active area of mathematics and engineering research since the seminal paper on the homogenization method by Bendsøe and Kikuchi [2]. In the past few decades, a number of different topology optimization methods have been proposed and applied to various engineering problems [24, 7, 26]. Topology optimization methods can be classified into two groups by the way they represent the structural domain $\Omega \subset \mathbb{R}^d$: density-based methods and level-set-based methods. In the present work, we focus on level-set methods, which represent the domain Ω implicitly using the level-set function ϕ defined over the entire working domain and provides crisp boundary representation of structures undergoing topology changes [26].

*Corresponding author

Email addresses: aaron.klein@mail.utoronto.ca (Aaron Klein), pbn@utias.utoronto.ca (Prasanth B. Nair), masa.yano@utoronto.ca (Masayuki Yano)

One of the key ingredients of level-set-based topology optimization is the shape derivative, which characterizes the change in the objective function $J(\Omega)$ with respect to the change in the geometry Ω. In the present work we formally denote the shape derivative as a directional derivative $dJ(\Omega;\cdot)$, where the second argument specifies the direction about which the derivative is evaluated. There are two distinct approaches to evaluate the shape derivative $dJ(\Omega;\cdot)$: a boundary-based shape derivative $dJ^{\mathrm{Bdry}}(\Omega;\cdot)$ and a volumetric shape derivative $dJ^{\mathrm{Vol}}(\Omega;\cdot)$.

The majority of level-set topology optimization methods use boundary-based shape derivative expressions [26] to compute the descent direction. This method to obtain a boundary-based shape derivative was first proposed by Hadamard [15]. This method was formalized for shape optimization by Delfour and Zolesio [9] and was later used for level-set topology optimization by Wang et al. [28] and Allaire et al. [1]. While popular, the expression for $dJ^{\mathrm{Bdry}}(\Omega;\cdot)$ formally assumes that both the domain shape and the associated solution are sufficiently regular in the sense that $\partial\Omega$ is twice continuously differentiable and the solution is in $H^2(\Omega)^d$ [1]; neither of these requirements are strictly satisfied for standard finite element implementations. In addition, for scalar elliptic equations with Dirichlet boundary conditions, Hiptmair et al. [16] have shown that the piecewise linear finite element approximation of $dJ^{\mathrm{Bdry}}(\Omega;\cdot)$ is only first-order accurate in the finite element mesh spacing parameter h.

An alternative to boundary-based shape derivative is volumetric (or distributed) shape derivative. Early works on volumetric shape derivative include [8] [17, Section 3.3.7], as discussed in [9, Chapter 1, Section 5]. More recently, following the analysis of volumetric and boundary-based shape derivatives by Hiptmair et. al [16], volumetric shape derivatives have been developed for various optimization problems, including Stokes equation [30], electric motors [13], linear elasticity [11], fluid–structure interaction [12], and eigenvalue problems [29, 31]. The averaged adjoint method was developed as a framework to develop the shape derivatives in distributed/weak form for general PDE constrained optimization problems. The method was originally introduced by Sturm [25], further developed in Laurain and Sturm [21], and later extended to linear elasticity problems by Laurain [18]. Since the distributed shape derivative yields volumetric (as opposed to boundary-based) expressions for objective functions of our interest, we refer to them as volumetric shape derivatives throughout this work. The two shape derivative expressions $dJ^{\mathrm{Bdry}}(\Omega;\cdot)$ and $dJ^{\mathrm{Vol}}(\Omega;\cdot)$ yield identical results if $\partial\Omega$ is smooth and the linear elasticity equation is solved exactly. However, the expression for $dJ^{\mathrm{Vol}}(\Omega;\cdot)$ places weaker regularity requirements than boundary-based derivatives; it only assumes $\partial\Omega$ is Lipschitz continuous and the solution is in $H^1(\Omega)^d$, both of which are satisfied for typical finite element analysis. In addition, for scalar elliptic equations, Hiptmair et al. [16] have shown that the piecewise linear finite element approximation of $dJ^{\mathrm{Vol}}(\Omega;\cdot)$ is second-order accurate in h under regularity assumptions that

[1] Throughout this work, $H^q(\Omega)$ denotes the Sobolev space of functions with weak derivatives up to order q that are square integrable.

are often satisfied.

The twofold contributions of this work are the theoretical analyses and numerical comparisons of the two shape derivative expressions for linear objective functionals arising in linear elasticity problems. We first develop a pair of theorems that show that, for sufficiently regular problems, the finite element approximations of the boundary-based and volumetric shape derivatives are k-th and $2k$-th order accurate, where k is the polynomial degree of the elements, respectively; the result is an extension of [16] for piecewise linear finite element approximation of scalar elliptic equations to degree-k finite element approximation of linear elasticity equations. In addition to the analysis of the shape derivatives, we also develop theorems that show the finite element approximations for descent directions with common velocity extension/smoothing formulations. The descent direction based on the boundary-based shape derivative is k-th order accurate in both H^1 and L^2 norms, whereas that based on the volumetric shape derivative is k-th and $k+1$ order accurate in the H^1 and L^2 norm, respectively. We next assess, using numerical examples, the performance of the topology optimization methods based on the two shape derivative expressions for practical topology optimization problems; we demonstrate that the weaker regularity requirement and higher-order accuracy of the volumetric shape derivative expression provide practical benefits.

This paper is organized as follows. In Section 2, we introduce the topology optimization problem considered throughout this work and highlight the role of the shape derivative. In Section 3, we introduce the boundary-based and volumetric shape derivative expressions. In Section 4, we analyze the error in the finite element approximations of the shape derivative expressions. In Section 5, we first verify the *a priori* error bounds using a simple numerical example; we then assess the implications of the choice of the shape derivatives in a practical topology optimization test problem.

2. Problem statement

In this section, we define the level-set-based approach to topology optimization that we consider throughout this work. To this end, we introduce a d-dimensional working domain $\mathcal{D} \subset \mathbb{R}^d$ that contains all possible structural domains for $d \in \{2, 3\}$. We next introduce a level-set function $\phi : \mathcal{D} \to \mathbb{R}$ defined over the entire working domain $\mathcal{D}$. The structural domain $\Omega \subset \mathcal{D}$ is then implicitly defined by the level-set function:

$$\Omega \coloneqq \{x \in \mathcal{D} \mid \phi(x) < 0\}.$$

We next introduce the linear elasticity problem. The isotropic linear elasticity problem over the (level-set-represented) domain $\Omega \subset \mathbb{R}^d$ is given by

$$\begin{aligned} -\operatorname{div}(Ke(u)) &= f \quad \text{in } \Omega, \\ u &= 0 \quad \text{on } \Gamma_D, \\ (Ke(u)) \cdot n &= g \quad \text{on } \Gamma_N, \end{aligned} \tag{1}$$

where $\partial\Omega = \overline{\Gamma}_N \cup \overline{\Gamma}_D$, $\Gamma_N \subset \partial\Omega$ is the Neumann boundary, $\Gamma_D \subset \partial\Omega$ is the Dirichlet boundary, n is the outward pointing normal on $\partial\Omega$, $g : \Gamma_N \to \mathbb{R}^d$ is the traction force, $f : \mathcal{D} \to \mathbb{R}^d$ is the body force, $u : \Omega \to \mathbb{R}^d$ is the displacement, $e(u) = \frac{1}{2}(Du + Du^T)$ is the strain tensor field, D is the gradient operator on a vector field, and K is the stiffness tensor such that $KX = 2\tilde{\mu}X + \tilde{\lambda}\mathrm{Tr}(X)I$ for any $X \in \mathbb{R}^{d\times d}$, where $\tilde{\lambda}$ and $\tilde{\mu}$ are the Lamé coefficients, which satisfy $\tilde{\mu} \geq \tilde{\mu}_{\min} > 0$ and $\tilde{\lambda} \geq 0$. (*Note:* while we do not explicitly indicate the dependence of u on Ω, throughout this paper it should be understood that u is associated with a particular Ω.)

We next introduce the weak form of (1). To this end, we introduce a Hilbert space $\mathcal{U}(\Omega) \coloneqq \{u \in H^1(\Omega)^d \mid u|_{\Gamma_D} = 0\}$. The weak statement is as follows: find $u \in \mathcal{U}(\Omega)$ such that

$$a(u, v) = \ell(v) \quad \forall v \in \mathcal{U}(\Omega), \tag{2}$$

where

$$\begin{aligned} a(w, v) &\coloneqq \int_\Omega Ke(w) : e(v)\mathrm{d}x \quad \forall w, v \in \mathcal{U}(\Omega), \\ \ell(v) &\coloneqq \int_\Omega f \cdot v\mathrm{d}x + \int_{\Gamma_N} g \cdot v\mathrm{d}s \quad \forall v \in \mathcal{U}(\Omega), \end{aligned}$$

where $A : B$ denotes the Frobenius inner product of tensors A and B. We assume that $\Gamma_D \neq \emptyset$, $f \in H^{-1}(\mathcal{D})^d$, $g \in L^2(\Gamma_N)^d$, $\tilde{\lambda} \in L^\infty(\Omega)$, and $\tilde{\mu} \in L^\infty(\Omega)$, so that the bilinear form $a : \mathcal{U}(\Omega) \times \mathcal{U}(\Omega) \to \mathbb{R}$ is coercive and continuous and the linear form $\ell \in \mathcal{U}(\Omega)'$ is continuous. The weak problem is hence well-posed by the Lax-Milgram theorem [3]. In practice we approximate the solution in a finite-dimensional subspace $\mathcal{U}_h(\Omega) \subset \mathcal{U}(\Omega)$ using a finite element method.

We now introduce objective functions that are of interest in structural topology optimization problems. In the present work, we consider linear functionals of the form

$$J(\Omega) \coloneqq \int_\Omega j_v \cdot u\mathrm{d}x + \int_{\Gamma_N} j_b \cdot u\mathrm{d}s + \lambda V(\Omega), \tag{3}$$

where $j_v : \mathcal{D} \to \mathbb{R}^d$ is defined over the volume, $j_b : \Gamma_N \to \mathbb{R}^d$ is defined over the Neumann boundary, $V(\Omega)$ is the volume of the structure Ω, and $\lambda \in \mathbb{R}_{>0}$ is the volume penalization constant. (Again, u should be understood to be associated with the particular Ω.) This general form of linear functional encapsulates many functionals of practical interest. One commonly studied objective function is volume penalized compliance

$$J_{\mathrm{comp}}(\Omega) \coloneqq \int_\Omega f \cdot u\mathrm{d}x + \int_{\Gamma_N} g \cdot u\mathrm{d}s + \lambda V(\Omega) = \int_\Omega Ke(u) : e(u)\mathrm{d}x + \lambda V(\Omega),$$

which is a measure of the internal energy of the structure under load and is useful for rigidity maximization. Another functional of potential interest is the average displacement in the direction $c \in \mathbb{R}^d$ over a select region $\omega \subset \Omega$,

$$J_{\mathrm{disp}}(\Omega) \coloneqq \int_\Omega \chi_\omega c \cdot u dx + \lambda V(\Omega),$$

where $\chi_\omega : \Omega \to \mathbb{R}_{\geq 0}$ is the characteristic function associated with the region of interest ω. (We assume that the direction $c \in \mathbb{R}^d$ is chosen such that the integral is positive for the given load.) While we embed the volume penalty in the objective function in the present work, this term could be treated as an explicit constraint and incorporated in the "objective function" using, for example, an augmented Lagrangian method [1, 4, 27].

Before we introduce our optimization problem, we state our key assumption:

Assumption 1. *Throughout this work, we assume that the following surfaces are part of $\partial\mathcal{D}$ and are fixed: (i) the Dirichlet boundary Γ_D, (ii) the part of the Neumann boundary with finite traction $\{x \in \Gamma_N \mid g(x) \neq 0\}$, and (iii) the part of Neumann boundary with finite output $\{x \in \Gamma_N \mid j_b(x) \neq 0\}$. In other words, these three parts of the boundary are always included in the structure boundary $\partial\Omega$.*

Many practical topology optimization problems satisfy Assumption 1 because the support and loading surfaces of the structures are typically prescribed.

We now state the topology optimization problem: find $\Omega^\star$ such that

$$\Omega^\star \equiv \arg\min_{\Omega \subset \mathcal{D}} J(\Omega). \tag{4}$$

This optimization problem is solved using a gradient-based method. Specifically, we evolve the geometry Ω based on the gradient of $J(\Omega)$ with respect to Ω: i.e., the *shape derivative* $dJ(\Omega, \cdot)$. The successful solution of the topology optimization problem (4) relies on an accurate evaluation of the shape derivative $dJ(\Omega, \cdot)$, which informs a descent direction. In the following sections, we (i) introduce formulations to evaluate the shape derivative $dJ(\Omega, \cdot)$, (ii) provide *a priori* error analyses of the accuracy of the finite element approximation of $dJ(\Omega, \cdot)$, and (iii) demonstrate their impact in practical topology optimization problems.

3. Shape derivatives: formulation

3.1. Preliminary

In this section, we present two different approaches to evaluate shape derivatives. To begin, we formalize the concept of shape derivative following [21, 18]. We first introduce a vector space of all admissible deformations

$$\Theta(\mathcal{D}) \coloneqq \{\theta \in W^{1,\infty}(\mathcal{D})^d \mid \theta \cdot n = 0 \text{ on } \partial\mathcal{D}\}$$

on the working domain $\mathcal{D} \subset \mathbb{R}^d$.[2] We next consider a vector field $\theta \in \Theta(\mathcal{D})$ and the associated flow $\Phi_t^\theta : \mathcal{D} \to \mathbb{R}^d$, $t \in [0, \tau]$, that maps each $x^0 \in \mathcal{D}$ to $x(t) \coloneqq \Phi_t^\theta(x^0)$, where $x(t)$ is the solution to $\dot{x}(t) = \theta(x(t))$

[2] Throughout this work, $W^{k,p}(\mathcal{D})$ denotes the space of functions whose weak derivatives up to order k are in $L^p(\mathcal{D})$.

with the initial condition $x(t=0) = x^0$. The associated family of deformed domains is given by $\Omega_t \coloneqq \Phi_t^\theta(\Omega)$, $t \in [0, \tau]$. The *shape derivative* of J at Ω is the linear continuous operator $dJ(\Omega; \cdot) : \Theta(\mathcal{D}) \to \mathbb{R}$ such that

$$dJ(\Omega;\theta) = \lim_{t \searrow 0} \frac{1}{t}(J(\Omega_t) - J(\Omega)) \quad \forall \theta \in \Theta(\mathcal{D}).$$

We now review two distinct expressions for the shape derivative: the boundary-based shape derivative and the volumetric shape derivative.

3.2. Boundary-based shape derivative

We present the boundary-based shape derivative in [1], which, as discussed in the introduction, is used in the majority of level-set topology optimization methods. For completeness, the derivation is included in Appendix A. To begin, we introduce the adjoint problem: find $p \in \mathcal{U}(\Omega)$ such that

$$\int_\Omega Ke(p) : e(\hat{\varphi}) \mathrm{d}x = -\int_\Omega j_v \cdot \hat{\varphi} \mathrm{d}x - \int_{\Gamma_N} j_b \cdot \hat{\varphi} \mathrm{d}s \quad \forall \hat{\varphi} \in \mathcal{U}(\Omega). \tag{5}$$

We assume the linear elasticity problem (2) and the adjoint problem (5) satisfy the following regularity conditions: $\partial\Omega \in \mathcal{C}^2$, $f \in L^2(\Omega)^d$, $g \in H^2(\mathcal{D})^d$, $j_v \in L^2(\Omega)^d$, $j_b \in H^2(\mathcal{D})^d$, $u \in H^2(\Omega)^d$, and $p \in H^2(\Omega)^d$. Under these conditions, the boundary-based shape derivative for the first part of the linear objective functional (3) is given by

$$\begin{aligned} dJ^{\mathrm{Bdry}}(\Omega;\theta) \coloneqq &\int_{\Gamma_\mathrm{N}} \theta \cdot n \left[j_v \cdot u + Ke(u) : e(p) - p \cdot f - \frac{\partial (g \cdot p)}{\partial n} - Mg \cdot p \right] \mathrm{d}s \\ &+ \int_{\Gamma_\mathrm{D}} \theta \cdot n \left[j_v \cdot u - Ke(u) : e(p) \right] \mathrm{d}s + \int_{\partial\Omega} \theta \cdot n \left[\frac{\partial (j_b \cdot u)}{\partial n} + M j_b \cdot u \right] \mathrm{d}s, \end{aligned}$$

where M is the curvature of $\partial\Omega$, which may be expressed as $M = \operatorname{div} n$ for $n = \nabla\phi / \|\nabla\phi\|$. Under Assumption 1, the shape derivative simplifies to

$$dJ^{\mathrm{Bdry}}(\Omega;\theta) \coloneqq \int_{\Gamma_\mathrm{N}} \theta \cdot n \left[j_v \cdot u + Ke(u) : e(p) - p \cdot f \right] \mathrm{d}s. \tag{6}$$

The boundary-based shape derivative of the volume penalty, $V(\Omega) \coloneqq \int_\Omega \mathrm{d}x$, is given by

$$dV^{\mathrm{Bdry}}(\Omega;\theta) \coloneqq \int_{\partial\Omega} \theta \cdot n \mathrm{d}s.$$

Remark 1. *For (6) to be a valid formulation, we require that $\partial\Omega \in \mathcal{C}^2$. While the condition may hold for a continuous representation of the structure Ω, the condition in general does not hold for the discrete approximation of Ω associated with piecewise polynomial level sets.*

Remark 2. *Suppose (i) there is no body force (i.e., $f = 0$) and (ii) the objective function is the compliance (i.e., $j_b = g$ and $j_v = f = 0$). Then the problem is self-adjoint, the adjoint state is $p = -u$, and the boundary-based shape derivative simplifies to*

$$dJ^{\mathrm{Bdry}}(\Omega;\theta) = \int_{\Gamma_\mathrm{N}} \left[-Ke(u) : e(u) \right] \theta \cdot n \mathrm{d}s. \tag{7}$$

3.3. Volumetric shape derivative

We next present the volumetric shape derivative expressions in [18]. For completeness, the derivation is included in Appendix B. Under Assumption 1, the volumetric shape derivative for the first part of the linear objective functional (3) is given by

$$\begin{aligned} dJ^{\mathrm{Vol}}(\Omega;\theta) \coloneqq &- \int_\Omega (Du^T Ke(p) + Dp^T Ke(u)) : D\theta \mathrm{d}x + \int_\Omega Ke(u) : e(p) \operatorname{div}\theta \mathrm{d}x \\ &+ \int_\Omega (\partial_x j_v \cdot u) \cdot \theta \mathrm{d}x + \int_\Omega j_v \cdot u \operatorname{div}\theta \mathrm{d}x - \int_\Omega (\partial_x f \cdot p) \cdot \theta \mathrm{d}x - \int_\Omega f \cdot p \operatorname{div}\theta \mathrm{d}x, \end{aligned} \tag{8}$$

where $\partial_x j_v$ and $\partial_x f$ are the spatial gradients of j_v and f, respectively, and $u \in \mathcal{U}(\Omega)$ and $p \in \mathcal{U}(\Omega)$ are the solutions to (2) and (5), respectively. The volumetric shape derivative of the volume penalty is given by

$$dV^{\mathrm{Vol}}(\Omega;\theta) \coloneqq \int_\Omega \operatorname{div}\theta \mathrm{d}x.$$

Remark 3. *Suppose (i) there is no body force (i.e., $f = 0$) and (ii) the objective function is the compliance output (i.e., $j_b = g$ and $j_v = f = 0$). Then the problem is self-adjoint, the adjoint state is $p = -u$, and the volumetric shape derivative simplifies to*

$$dJ^{\mathrm{Vol}}(\Omega;\theta) = \int_\Omega 2Du^T Ke(u) : D\theta - Ke(u) : e(u) \operatorname{div}\theta \mathrm{d}x. \tag{9}$$

Remark 4. *If $\partial\Omega \in \mathcal{C}^1$, the divergence theorem yields*

$$dV^{\mathrm{Vol}}(\Omega;\theta) \coloneqq \int_\Omega \operatorname{div}\theta \mathrm{d}x = \int_{\partial\Omega} \theta \cdot n \mathrm{d}s =: dV^{\mathrm{Bdry}}(\Omega;\theta);$$

i.e., we recover the boundary-based shape derivative for the volume penalty term. However, this equivalence does not hold for $\partial\Omega \notin \mathcal{C}^1$.

3.4. Shape derivatives in topology optimization: practical aspects

We have introduced two different shape derivative expressions. These expressions in principle allow us to define the steepest descent direction $\theta^\star = \arg\min_\theta dJ(\Omega;\theta)$. However, the steepest descent direction defined in this manner would not be unique because the shape derivatives depend on θ over only a part of the working domain $\mathcal{D}$ and not the whole $\mathcal{D}$. Namely, the boundary-based shape derivative depends only on $(\theta \cdot n)|_{\partial\Omega}$ and the volumetric shape derivative depends only on $\theta|_\Omega$. To update our level-set function, we need the descent direction θ to be defined over the entire working domain $\mathcal{D}$.

While there are a number of approaches to extend the descent direction, a smooth extension has been shown to improve convergence of the optimization process [18, 4, 6]. One way to construct such an extension is to solve a smoothing PDE [21, 18, 6], which may be interpreted as finding a Riesz representation of the shape derivative $dJ(\Omega;\cdot)$ in an appropriate space [23]. Namely, we first introduce a space $\mathcal{V}(\mathcal{D}) \equiv \{\theta \in H^1(\mathcal{D})^d \mid \theta \cdot n|_{\partial\mathcal{D}} = 0\}$ endowed with an inner product $(\cdot,\cdot)_{\mathcal{V}} : \mathcal{V}(\mathcal{D}) \times \mathcal{V}(\mathcal{D}) \to \mathbb{R}$ such that

$$(w,v)_{\mathcal{V}} \coloneqq \int_{\mathcal{D}} (Dw : Dv + \alpha w \cdot v) dx \quad \forall w, v \in \mathcal{V}(\mathcal{D})$$

for some $\alpha \in \mathbb{R}_{>0}$, and the associated induced norm $\|v\|_{\mathcal{V}} \coloneqq \sqrt{(v,v)_{\mathcal{V}}}$. We then solve for the Riesz representation: find $\theta^\star \in \mathcal{V}(\mathcal{D})$ such that

$$(\theta^\star, \xi)_{\mathcal{V}} = -dJ(\Omega;\xi) \quad \forall \xi \in \mathcal{V}(\mathcal{D}). \tag{10}$$

This extension and regularization method has been shown to provide improved convergence for an eigenvalue topology optimization problem with a boundary based shape derivative by de Gournay [6] and has been applied in conjunction with volumetric shape derivatives by Laurain [18]. Laurain [18] considers parameter of $\alpha = 1/10$. The smooth extension mitigates oscillating or irregular boundaries that might arise from less smooth extensions.

Given the smoothed descent direction $\theta^\star : \mathcal{D} \to \mathbb{R}^d$, we evolve the level-set function $\phi : \mathcal{D} \to \mathbb{R}$ using a linear advection equation [18]

$$\frac{\partial \phi}{\partial t} + \theta^\star \cdot \nabla \phi = 0. \tag{11}$$

In practice, at each optimization iteration, the level-set function is advected in the descent direction for a given time interval Δt, which may be found through a line search procedure [1, 18]. The line search procedure involves checking the objective function $J(\Omega)$ after every iteration to ensure it decreases. If $J(\Omega)$ has increased after Ω has been updated through the linear advection equation (11), the time step Δt is reduced, and Ω is recalculated. This procedure is repeated until the objective function decreases, or the maximum number of linesearch steps have been attempted, at which point the structure Ω is accepted for the next iteration, and the optimization process proceeds.

In principle the above approach to compute descent directions works for both volumetric and boundary-based shape derivative expressions. In fact, based on [20, Propositions 1], under suitable regularity assumptions, we may express the boundary-based derivative (7) in a volumetric form $dJ^{\text{Bdry}}(\Omega;\theta) = \int_\Omega (S : D\theta + \operatorname{div}(S)\cdot\theta)\mathrm{d}x$ with $S = -Ke(u) : e(u) I$. Furthermore, [20, Proposition 2] states that there are numerous such expressions; we may replace S with any $\hat{S}$ such that $\hat{S}n = Sn$ on $\partial\Omega$. However, many practical implementations based on the boundary-based shape derivative uses a different formulation to compute the descent direction [26, 1, 4]. For compliance minimization problems under Assumption 1, we recall that the boundary-based shape derivative is $dJ^{\text{Bdry}}(\Omega;\theta) = \int_{\Gamma_N} \theta \cdot n \left[-Ke(u) : e(u)\right] \mathrm{d}s$. Many practical implementations "naturally extend", without a mathematical justification, the integrand of boundary integral as a volumetric integrand to introduce

$$\widetilde{dJ}^{\text{Bdry}}(\Omega;v) = \int_\Omega \left[-Ke(u) : e(u)\right] v \mathrm{d}x, \tag{12}$$

for $v \in H^1(\Omega)$. This "natural extension" provides two main benefits: first, it removes the need for finite elements that conform to the boundary of the structure, $\partial\Omega$. This enables the use of fixed grid approaches. Second, it reduces the regularity requirements on the finite element approximation space, from $u_h \in H^2(\Omega)$ for (7) to $u_h \in H^1(\Omega)$ for (12). The reduction in regularity required for u_h is of particular importance for

practical topology optimization, as the regularity requirements for (7) are not strictly satisfied by linear finite elements.

To find the descent direction, we then compute the Riesz representation of this "naturally extended" functional $\widetilde{dJ}^{\text{Bdry}}(\Omega;\cdot)$: find $\zeta^\star \in H^1(\Omega)$ such that

$$\int_{\mathcal{D}} (\nabla\zeta^\star \cdot \nabla v + \alpha\zeta^\star v)dx = \widetilde{dJ}^{\text{Bdry}}(\Omega; v) \quad \forall v \in H^1(\Omega) \tag{13}$$

for some $\alpha \in \mathbb{R}_{>0}$. Given the smoothed scalar descent direction $\zeta^\star : \mathcal{D} \to H^1(\mathcal{D})$, we evolve the level-set function $\phi : \mathcal{D} \to \mathbb{R}$ using the Hamilton-Jacobi equation [1, 22]

$$\frac{\partial\phi}{\partial t} + \zeta^\star|\nabla\phi| = 0. \tag{14}$$

In this work, we consider the above to be the "practical implementation" of topology optimization methods based on boundary-based shape derivatives.

The level set evolution by (11) or (14) in general does not maintain the signed-distance property, $|\nabla\phi| = 1$, and can become too flat or too steep. To address the problem, it is standard practice to perform a "reinitialization step" every few iterations [1, 18, 4]. Namely, starting with the initial level ϕ_0, we reinitialize by solving the time-relaxed Eikonal equation

$$\begin{aligned} \frac{\partial\phi}{\partial t} + \text{sign}(\phi_0)(|\nabla\phi| - 1) = 0 \quad &\text{in } \mathcal{D} \times \mathbb{R}_{>0}, \\ \phi(t = 0, x) = \phi_0(x) \quad &\text{on } \mathcal{D} \end{aligned} \tag{15}$$

to steady state. Note that the steady state solution satisfies $|\nabla\phi| = 1$ and hence is a signed-distance function.

We summarize the level-set topology optimization algorithm that incorporates the above ingredients in Algorithm 1. We will study the impact of the choice of three algorithmic parameters—the smoothing parameter α, the advection time interval Δt, and whether to reinitialize—in Section 5.2.

3.5. Topology optimization with ersatz material

In practice, level-set topology optimization algorithms commonly use ersatz material [26, 1, 18]. The idea is (i) to place weak material with the stiffness tensor $K_\epsilon := \epsilon K$, $\epsilon \ll 1$, in the region outside of the structure $\mathcal{D} \setminus \Omega$; (ii) to restate the the linear elasticity problem (1) over the working domain $\mathcal{D}$; and (iii) to obtain the solution u_ϵ, which approximates u in Ω. Dambrine et al. [5] have shown that u_ϵ converges to u, as $\|u - u_\varepsilon\|_{\text{H}^1(\Omega)} \leq C(\Omega, \mathcal{D}, f, g)\varepsilon$ for scalar elliptic problems.

Laurain [19][3] analyzes the effect of ersatz materials on the shape derivatives for linear elasticity problems. The volumetric shape derivative (8), with integrals defined over the working domain $\mathcal{D}$ instead of Ω, is valid

[3]The manuscript [19] is the version of [18] on arXiv, which includes Section 3.7 that is removed in the final published work.

Algorithm 1: Level-set topology optimization algorithm.

inputs : initial level set: ϕ^0

outputs: final level set: $\phi^{N_{\max}}$

for $N = 1, \ldots, N_{\max}$ **do**
  Solve the linear elasticity problem (2) on Ω implied by ϕ^N.
  Evaluate the shape derivative $dJ^{\mathrm{Vol/Bdry}}(\Omega; \cdot)$ using (6) or (8).
  Compute the descent direction extension $\theta^\star$ or $\zeta^\star$ using (10) or (13).
  for $N_{\mathrm{line}} = 1, \ldots, N_{\mathrm{line,max}}$ **do**
    Evolve the level set function from ϕ^N to ϕ^{N+1} using the advection equation (11) or (14) with timestep Δt.
    if $J(\phi^{N+1}) < J(\phi^N)$ **then**
      break.
    else
      Reduce the timestep to $\Delta t \leftarrow \beta \Delta t$ for a prescribed $\beta \in (0, 1)$.
    end
  end
  if $\mathrm{mod}(N, N_{\mathrm{reinit}}) = 0$ **then**
    Reinitialize the level set ϕ^{N+1} using the time-relaxed Eikonal equation (15).
  end
end

for linear objective functionals (including compliance) regardless of the value of ϵ [19]. On the other hand, the boundary-based shape derivative for a compliance objective takes on the form

$$dJ^{\mathrm{Bdry}_\epsilon}(\Omega;\theta) = \int_{\partial\Omega} \left(2K_\epsilon e\left(u_\epsilon^-\right) n \cdot [\![Du_\epsilon]\!] n\right) \theta \cdot n \mathrm{d}s - \int_{\partial\Omega} [\![Ke(u_\epsilon) : e(u_\epsilon)]\!] \theta \cdot n \mathrm{d}s, \tag{16}$$

where $(\cdot)^-$ denotes the restriction to the void region $\mathcal{D} \setminus \Omega$, and $[\![\cdot]\!]$ denotes the jump in a function across the boundary $\partial\Omega$. The differences in the original boundary-based shape derivative (7) and the shape derivative (16) are (i) the addition of the first integral $\int_{\partial\Omega} \left(2K_\epsilon e\left(u_\epsilon^-\right) n \cdot [\![Du_\epsilon]\!] n\right) \mathrm{d}s$ and (ii) the subtraction of $K_\epsilon e(u_\epsilon^-) : e(u_\epsilon^-)$ from the second integral effected by the jump operator. In practice, due to the ease of implementation, the original shape derivative (7) is often used even when the ersatz approximation is used to yield the displacement field u_ϵ. In addition, while the ersatz material method introduces additional errors to the approximations of the true displacement field u, in practice they provide (arguably favorable) smoothing of the descent direction when performing topology optimization.

4. Shape derivatives: *a priori* error analysis

4.1. Preliminaries

We now analyze the accuracy of the finite element approximation of the two shape derivatives: the volumetric shape derivative (8) and the boundary-based shape derivative (6). Hiptmair et al. [16] provides, to the best of our knowledge, the first analysis of the piecewise linear finite element approximation errors on the shape derivatives for scalar elliptic PDEs with linear objective functionals. We present here an extension of the analysis to degree-k finite element approximations of linear elasticity problems with linear objective functionals.

By way of preliminaries, we provide a few assumptions that we consider throughout the analysis.

Assumption 2 (finite element space and approximation)**.** *Let*

$$\mathcal{U}_h(\Omega) \coloneqq \left\{ v \in \mathcal{U}(\Omega) \mid v|_{\mathcal{K}} \in \mathbb{P}^k(\mathcal{K})^d, \forall \mathcal{K} \in \mathcal{T}_h \right\}, \tag{17}$$

where $\mathcal{T}_h$ is the triangulation of Ω that comprises elements $\{\mathcal{K}\}$ such that $\max_{\mathcal{K}\in\mathcal{T}_h} \mathrm{diam}(\mathcal{K}) = h$, and $\mathbb{P}^k(\mathcal{K})$ is the space of degree $k \geq 1$ polynomials on $\mathcal{K}$. The finite element approximation of the linear elasticity problem (2) is $u_h \in \mathcal{U}_h(\Omega)$ such that

$$a(u_h, v) = \ell(v) \quad \forall v \in \mathcal{U}_h(\Omega).$$

The finite element approximation of the adjoint problem (5) is $p_h \in \mathcal{U}_h(\Omega)$ such that

$$a(w, p_h) = -\int_\Omega j_v \cdot w \mathrm{d}x - \int_{\Gamma_N} j_b \cdot w \mathrm{d}s \quad \forall w \in \mathcal{U}_h(\Omega).$$

Both finite element problems are well-posed by the Lax-Milgram theorem.

Assumption 3 (elliptic regularity estimate)**.** *Consider the linear elasticity problem* (2)*. Let* $w \in \mathcal{U}(\Omega)$ *satisfy*

$$\int_\Omega Ke(w) : e(v)\mathrm{d}x = \int_\Omega \rho \cdot v\mathrm{d}s \quad \forall v \in \mathcal{U}(\Omega)$$

for $\rho \in H^{k-1}(\Omega)^d$*. Then* $w \in H^{k+1}(\Omega)^d$ *and there exists a constant* C_r *that depends only on* Ω *such that*

$$\|w\|_{H^{k+1}(\Omega)} \leq C_r \|\rho\|_{H^{k-1}(\Omega)}.$$

Assumption 4 (regularity of solution and adjoint)**.** *In the linear elasticity problem* (2)*, we assume that* Ω*,* f *and* g *are sufficiently regular such that* u *is in* $H^{k+1}(\Omega)^d$*. In the adjoint problem* (5)*, we assume* Ω*,* j_v*, and* j_b *are sufficiently regular such that* p *is in* $H^{k+1}(\Omega)^d$*.*

Remark 5. *Assumption 4* assumes *that domain* Ω *is sufficient regular so that the state* u *and adjoint* p *are in* $H^{k+1}(\Omega)^d$*. In practice, domains encountered in topology optimization are only piecewise smooth, and these assumptions may be violated. A complete analysis of the regularity of the domain on the accuracy of the volumetric and boundary-based derivative is beyond the scope of this work. However, we numerically observe in Section 5 that, at least for some piecewise smooth domains, the optimal convergence rate is achieved. We also refer to [20] for a recent analysis of shape derivatives in nonsmooth domains.*

We now state a few standard finite element approximation results. We omit proofs here for brevity and refer to standard finite element textbooks such as [3] and [10].

Lemma 6 (interpolation error)**.** *For the finite element space* (17)*, there exists a nodal interpolation operator* $\mathcal{I}_h : H^{k+1}(\Omega)^d \cap \mathcal{U}(\Omega) \to \mathcal{U}_h(\Omega)$ *such that*

$$\|w - \mathcal{I}_h w\|_{H^1(\Omega)} \leq Ch^k |w|_{H^{k+1}(\Omega)} \quad \forall w \in H^{k+1}(\Omega) \cap \mathcal{U}(\Omega) \quad \forall h, \tag{18}$$

where C *is a constant independent of* w *and* h*.*

Proof. See, for example, [10, Corollary 1.110]. □

Lemma 7 (finite element error)**.** *Under the regularity Assumption 4, the finite element solution* $u_h \in \mathcal{U}_h(\Omega)$ *and adjoint* $p_h \in \mathcal{U}_h(\Omega)$ *given in Assumption 2 satisfy*

$$\|u - u_h\|_{H^1(\Omega)} \leq Ch^k |u|_{H^{k+1}(\Omega)},$$
$$\|p - p_h\|_{H^1(\Omega)} \leq Ch^k |p|_{H^{k+1}(\Omega)}$$

for some constant C *independent of* u*,* p*, and* h*.*

Proof. The result follows from Céa's lemma and polynomial interpolation error bounds (e.g., [10, Corollary 1.109]) under the regularity Assumption 4. □

4.2. Volumetric shape derivative

We now state the main result of the section: the *a priori* error analysis of the finite element approximation of the volumetric shape derivative. Our analysis for linear elasticity problems follows closely the analysis for piecewise linear finite element approximations of Poisson's equation by Hiptmair et al. [16].

Theorem 8. *Let $u \in \mathcal{U}(\Omega)$ and $p \in \mathcal{U}(\Omega)$ be the solutions to (1) and (5), respectively, and $u_h \in \mathcal{U}_h(\Omega)$ and $p_h \in \mathcal{U}_h(\Omega)$ be the associated finite element approximations defined in Assumption 2. Then under Assumptions 2–4 and assuming $\theta \in W^{k+1,4}(\Omega)$, $f \in W^{k,4}(\Omega)$, and $j_v \in W^{k,4}(\Omega)$,*

$$|dJ(\Omega;\theta) - dJ_h^{\mathrm{Vol}}(\Omega;\theta)| \leq C\|\theta\|_{W^{k+1,4}(\Omega)} h^{2k},$$

where $dJ_h^{\mathrm{Vol}}(\Omega;\cdot)$ is the finite element approximation of the volumetric shape derivative (8), and C is a constant independent of h.

Proof. We first appeal to the definition of the volumetric shape derivative (8) and invoke the triangle inequality to split the error into seven parts:

$$\begin{aligned}
&|dJ(\Omega;\theta) - dJ^{\mathrm{Vol}}(\Omega, u_h, p_h;\theta)| \\
&\leq \left|\int_\Omega (Du^T Ke(p) - Du_h^T Ke(p_h)) : D\theta \mathrm{d}x\right| + \left|\int_\Omega (Dp^T Ke(u) - Dp_h^T Ke(u_h)) : D\theta \mathrm{d}x\right| \\
&\quad + \left|\int_\Omega (Ke(u) : e(p) - Ke(u_h) : e(p_h)) \operatorname{div}\theta \mathrm{d}x\right| + \left|\int_\Omega (j_v \cdot u - j_v \cdot u_h) \operatorname{div}\theta \mathrm{d}x\right| \\
&\quad + \left|\int_\Omega ((\partial_x j_v) \cdot u - (\partial_x j_v) \cdot u_h) \cdot \theta \mathrm{d}x\right| + \left|\int_\Omega (f \cdot p - f \cdot p_h) \operatorname{div}\theta \mathrm{d}x\right| \\
&\quad + \left|\int_\Omega ((\partial_x f) \cdot p - (\partial_x f) \cdot p_h) \cdot \theta \mathrm{d}x\right| \\
&\coloneqq \text{(I)} + \text{(II)} + \text{(III)} + \text{(IV)} + \text{(V)} + \text{(VI)} + \text{(VII)}.
\end{aligned} \tag{19}$$

We will bound the seven terms in order.

We first bound (I). To begin, we further split (I) into three terms:

$$\begin{aligned}
\text{(I)} \leq &\left|\int_\Omega D(u-u_h)^T Ke(p) : D\theta \mathrm{d}x\right| + \left|\int_\Omega Du^T Ke(p-p_h) : D\theta \mathrm{d}x\right| \\
&+ \left|\int_\Omega D(u-u_h)^T Ke(p-p_h) : D\theta \mathrm{d}x\right| \coloneqq \text{(I.1)} + \text{(I.2)} + \text{(I.3)}.
\end{aligned}$$

To bound (I.1), we use a duality trick. To this end, we appeal to the symmetry of $Ke(p)$ to obtain

$$\text{(I.1)} = \int_\Omega Ke(p) D\theta : D(u-u_h) \mathrm{d}x.$$

We next introduce $w \in \mathcal{U}(\Omega)$ such that

$$\int_\Omega e(w) : Ke(v) \mathrm{d}x = \int_\Omega Ke(p) D\theta : Dv \mathrm{d}x \quad \forall v \in \mathcal{U}(\Omega).$$

The strong form of the problem is

$$-\operatorname{div}(Ke(w)) = -\operatorname{div}(Ke(p) : D\theta) \quad \text{in } \Omega,$$

with homogeneous Dirichlet and Neumann boundary conditions on Γ_D and Γ_N. The successive application of the Hölder's inequality, along with the Sobolev embedding theorem, shows that the forcing function can be bounded as

$$\begin{aligned}\|\operatorname{div}(Ke(p) : D\theta)\|_{W^{k-1,2}(\Omega)} &\leq C(\|\theta\|_{W^{k+1,4}(\Omega)}\|p\|_{W^{k,4}(\Omega)} + \|\theta\|_{W^{1,\infty}(\Omega)}\|p\|_{H^{k+1}(\Omega)}) \\ &\leq C\|\theta\|_{W^{k+1,4}(\Omega)}\|p\|_{H^{k+1}(\Omega)}.\end{aligned}$$

Since the forcing term is in $W^{k-1,2}(\Omega)^d$, by the elliptic regularity estimate (Assumption 3), $w \in H^{k+1}(\Omega)^d$ and $\|w\|_{H^{k+1}(\Omega)} \leq C\|\theta\|_{W^{k+1,4}(\Omega)}\|p\|_{H^{k+1}(\Omega)}$. We next observe that

$$\begin{aligned}\text{(I.1)} &= \left|\int_\Omega Ke(p)D\theta : D(u-u_h)\mathrm{d}x\right| = \left|\int_\Omega e(w) : Ke(u-u_h)\mathrm{d}x\right| \\ &= \left|\int_\Omega e(w-\mathcal{I}_h w) : Ke(u-u_h)\mathrm{d}x\right| \leq C\left\|u-u_h\right\|_{H^1(\Omega)}\left\|w-\mathcal{I}_h w\right\|_{H^1(\Omega)},\end{aligned}$$

where the second equality follows from the definition of w and the fact $u - u_h \in \mathcal{U}(\Omega)$, the third equality follows from Galerkin orthogonality, and the inequality follows from the continuity of $a(\cdot,\cdot)$. We now invoke the finite element error bound (Lemma 7) and the interpolation error bound (Lemma 6 under $\|w\|_{H^{k+1}(\Omega)} \leq C\|\theta\|_{W^{k+1,4}(\Omega)}\|p\|_{H^{k+1}(\Omega)}$) to obtain

$$\text{(I.1)} \leq Ch^{2k}\|u\|_{H^{k+1}(\Omega)}\|p\|_{H^{k+1}(\Omega)}\|\theta\|_{W^{k+1,4}(\Omega)}.$$

To bound (I.2), we follow a similar argument using a duality trick. To this end, we rearrange the expression to obtain

$$\text{(I.2)} \coloneqq \int_\Omega Du^T Ke(p-p_h) : D\theta\mathrm{d}x = \int_\Omega (Du)(D\theta) : (Ke(p-p_h))\mathrm{d}x.$$

We next introduce $z \in \mathcal{U}(\Omega)$ such that

$$\int_\Omega e(z) : Ke(v)\mathrm{d}x = \int_\Omega (Du)(D\theta) : Ke(v)\mathrm{d}x \quad \forall v \in \mathcal{U}(\Omega).$$

The strong form of the problem is

$$-\operatorname{div}(Ke(z)) = -\frac{1}{2}\operatorname{div}(K((Du)(D\theta) + (D\theta)^T(Du)^T)) \quad \text{in } \Omega$$

with homogeneous boundary conditions on Γ_D and Γ_N; here, we have invoked $(Du)(D\theta) : (Ke(v)) = \frac{1}{2}K((Du)(D\theta) + (D\theta)^T(Du)^T) : Dv$. The forcing function is bounded by $\|\operatorname{div}(K((Du)(D\theta) + (D\theta)^T(Du)^T))\|_{W^{k-1,2}(\Omega)} \leq C\|\theta\|_{W^{k+1,4}(\Omega)}\|u\|_{H^{k+1}(\Omega)}$. Since the forcing

term is in $W^{k-1,2}(\Omega)^d$, by the elliptic regularity estimate (Assumption 3), $z \in H^{k+1}(\Omega)^d$ and $\|z\|_{H^{k+1}(\Omega)} \leq C\|\theta\|_{W^{k+1,4}(\Omega)}\|u\|_{H^{k+1}(\Omega)}$. We next observe that

$$\begin{aligned}
\text{(I.2)} &= \left|\int_\Omega (Du)(D\theta) : (Ke(p-p_h))\mathrm{d}x\right| = \left|\int_\Omega e(z) : Ke(p-p_h)\mathrm{d}x\right| \\
&= \left|\int_\Omega e(z-\mathcal{I}_h z) : Ke(p-p_h)\mathrm{d}x\right| \leq C\|p-p_h\|_{H^1(\Omega)}\|z-\mathcal{I}_h z\|_{H^1(\Omega)} \\
&\leq C' h^{2k}\|u\|_{H^{k+1}(\Omega)}\|p\|_{H^{k+1}(\Omega)}\|\theta\|_{W^{k+1,4}(\Omega)},
\end{aligned}$$

where the second equality follows from the definition of z and the fact $p-p_h \in \mathcal{U}(\Omega)$, the third equality follows from Galerkin orthogonality, the first inequality follows from the continuity of $a(\cdot,\cdot)$, and the last inequality follows from the finite element error bound (Lemma 7) and the interpolation error bound (Lemma 6 under $\|z\|_{H^{k+1}(\Omega)} \leq C\|\theta\|_{W^{k+1,4}(\Omega)}\|u\|_{H^{k+1}(\Omega)}$).

To bound (I.3), we observe

$$\begin{aligned}
\text{(I.3)} &\coloneqq \left|\int_\Omega D(u-u_h)^T Ke(p-p_h) : D\theta\mathrm{d}x\right| \leq \|\theta\|_{W^{1,\infty}}\left|\int_\Omega D(u-u_h)^T Ke(p-p_h)\mathrm{d}x\right| \\
&\leq C\|\theta\|_{W^{1,\infty}(\Omega)}\|u-u_h\|_{H^1(\Omega)}\|p-p_h\|_{H^1(\Omega)} \leq C' h^{2k}\|\theta\|_{W^{k+1,4}(\Omega)}\|u\|_{H^{k+1}(\Omega)}\|p\|_{H^{k+1}(\Omega)},
\end{aligned}$$

where the first equality follows from Hölder's inequality, the second inequality follows from the continuity of $a(\cdot,\cdot)$, and the the last inequality follows from the finite element error bound (Lemma 7) and the Sobolev embedding $W^{k+1,4}(\Omega) \subset W^{1,\infty}(\Omega)$.

We combine the bounds for (I.1), (I.2), and (I.3) to obtain

$$\text{(I)} \leq Ch^{2k}\|\theta\|_{W^{k+1,4}(\Omega)}\|u\|_{H^{k+1}(\Omega)}\|p\|_{H^{k+1}(\Omega)},$$

which is the desired $\mathcal{O}(h^{2k})$ bound.

The procedure used to bound (II) is identical to (I) with the exchange in the roles of u and p. We hence obtain a bound

$$\text{(II)} \leq Ch^{2k}\|\theta\|_{W^{k+1,4}(\Omega)}\|u\|_{H^{k+1}(\Omega)}\|p\|_{H^{k+1}(\Omega)},$$

which again is the desired $\mathcal{O}(h^{2k})$ bound.

We now analyze (III). To begin, we split the term into three parts:

$$\begin{aligned}
\text{(III)} &= \int_\Omega (Ke(u-u_h) : e(p))\operatorname{div}\theta\mathrm{d}x + \int_\Omega (Ke(u) : e(p-p_h))\operatorname{div}\theta\mathrm{d}x \\
&\quad - \int_\Omega (Ke(u-u_h) : e(p-p_h))\operatorname{div}\theta\mathrm{d}x \coloneqq \text{(III.1)} + \text{(III.2)} + \text{(III.3)}.
\end{aligned}$$

To bound (III.1), we again use a duality trick. To this end, we introduce $y \in \mathcal{U}(\Omega)$ such that

$$\int_\Omega e(y) : Ke(v)\mathrm{d}x = \int_\Omega Ke(v) : e(p)\operatorname{div}\theta\mathrm{d}x \quad \forall v \in \mathcal{U}(\Omega). \tag{20}$$

The strong form of the problem is

$$-\operatorname{div}(Ke(y)) = -\operatorname{div}(Ke(p)\operatorname{div}\theta) \quad \text{in } \Omega,$$

with homogeneous boundary conditions on Γ_D and Γ_N. The forcing function is bounded by $\|\operatorname{div}(Ke(p)\operatorname{div}\theta)\|_{W^{k-1,2}(\Omega)} \leq C\|\theta\|_{W^{k+1,4}(\Omega)}\|p\|_{H^{k+1}(\Omega)}$. Since the forcing term is in $W^{k-1,2}(\Omega)$, by the elliptic regularity estimate (Assumption 3), $y \in H^{k+1}(\Omega)^d$ and $\|y\|_{H^{k+1}(\Omega)} \leq C\|\theta\|_{W^{k+1,4}(\Omega)}\|p\|_{H^{k+1}(\Omega)}$. It hence follows that

$$\begin{aligned}
\text{(III.1)} &= \left|\int_\Omega (Ke(u-u_h) : e(p))\operatorname{div}\theta \mathrm{d}x\right| = \left|\int_\Omega e(y) : Ke(u-u_h)\mathrm{d}x\right| \\
&= \left|\int_\Omega e(y-\mathcal{I}_h y) : Ke(u-u_h)\mathrm{d}x\right| \leq C\left\|u-u_h\right\|_{H^1(\Omega)}\left\|y-\mathcal{I}_h y\right\|_{H^1(\Omega)} \\
&\leq C'h^{2k}\left\|\theta\right\|_{W^{k+1,4}(\Omega)}\left\|p\right\|_{H^{k+1}(\Omega)}\left\|u\right\|_{H^{k+1}(\Omega)},
\end{aligned}$$

where the second equality follows from the definition of y and the fact $u-u_h \in \mathcal{U}(\Omega)$, the third equality follows from Galerkin orthogonality, the first inequality follows from the continuity of $a(\cdot,\cdot)$, and the last inequality follows from the finite element error bound (Lemma 7) and the interpolation error bound (Lemma 6 under $\|y\|_{H^{k+1}(\Omega)} \leq C\|\theta\|_{W^{k+1,4}(\Omega)}\|p\|_{H^{k+1}(\Omega)}$).

The procedure used to bound (III.2) is identical to (III.1) with the exchange in the roles of u and p. We hence obtain $\text{(III.2)} \leq Ch^{2k}\left\|\theta\right\|_{W^{k+1,4}(\Omega)}\left\|p\right\|_{H^{k+1}(\Omega)}\left\|u\right\|_{H^{k+1}(\Omega)}$.

To bound (III.3), we observe

$$\begin{aligned}
\text{(III.3)} &= \left|\int_\Omega (Ke(u-u_h) : e(p-p_h))\operatorname{div}\theta \mathrm{d}x\right| \leq \left\|\theta\right\|_{W^{1,\infty}(\Omega)}\left|\int_\Omega (Ke(u-u_h) : e(p-p_h))\operatorname{div}\theta \mathrm{d}x\right| \\
&\leq C\left\|\theta\right\|_{W^{1,\infty}(\Omega)}\left\|u-u_h\right\|_{H^1(\Omega)}\left\|p-p_h\right\|_{H^1(\Omega)} \leq C'h^{2k}\left\|\theta\right\|_{W^{k+1,4}(\Omega)}\left\|u\right\|_{H^{k+1}(\Omega)}\left\|p\right\|_{H^{k+1}(\Omega)},
\end{aligned}$$

where the first equality follows from Hölder's inequality, the second inequality follows from the continuity of $a(\cdot,\cdot)$, and the last inequality follows from the finite element error bound (Lemma 7) and the Sobolev embedding $W^{k+1,4}(\Omega) \subset W^{1,\infty}(\Omega)$.

We combine the bounds for (III.1), (III.2), and (III.3) to obtain

$$\text{(III)} \leq Ch^{2k}\left\|\theta\right\|_{W^{k+1,4}(\Omega)}\left\|p\right\|_{H^{k+1}(\Omega)}\left\|u\right\|_{H^{k+1}(\Omega)},$$

which is the desired $\mathcal{O}(h^{2k})$ bound.

We next analyze (IV) and (V), again using a duality trick. We introduce $q \in \mathcal{U}(\Omega)$ such that

$$\int_\Omega e(q) : Ke(v)\mathrm{d}x = \int_\Omega j_v \cdot v \operatorname{div}\theta \mathrm{d}x \quad \forall v \in \mathcal{U}(\Omega).$$

The strong form of the problem is

$$-\operatorname{div}(Ke(q)) = j_v \operatorname{div}\theta \quad \text{in } \Omega$$

with homogeneous boundary conditions on Γ_D and Γ_N. The forcing function is bounded by $\|j_v \operatorname{div}\theta\|_{W^{k-1,2}(\Omega)} \leq C\|j_v\|_{W^{k-1,4}(\Omega)}\|\theta\|_{W^{k,4}(\Omega)}$. Since the forcing term is in $W^{k-1,2}(\Omega)$, by the elliptic regularity estimate (Assumption 3), $q \in H^{k+1}(\Omega)^d$ and $\|q\|_{H^{k+1}(\Omega)} \leq C\|\theta\|_{W^{k,4}(\Omega)}\|j_v\|_{W^{k-1,4}(\Omega)}$. We observe that

$$\begin{aligned}
\text{(IV)} &= \left|\int_\Omega (j_v \cdot (u-u_h))\operatorname{div}\theta \mathrm{d}x\right| = \left|\int_\Omega e(q) : Ke(u-u_h)\mathrm{d}x\right| \\
&= \left|\int_\Omega e(q-\mathcal{I}_h q) : Ke(u-u_h)\mathrm{d}x\right| \leq C\|u-u_h\|_{H^1(\Omega)}\|q-\mathcal{I}_h q\|_{H^1(\Omega)} \\
&\leq C' h^{2k}\|j_v\|_{W^{k-1,4}(\Omega)}\|\theta\|_{W^{k,4}(\Omega)}\|u\|_{H^{k+1}(\Omega)},
\end{aligned}$$

where the second equality follows from the definition of q and the fact $u-u_h \in \mathcal{U}(\Omega)$, the third equality follows from Galerkin orthogonality, the first inequality follows from the continuity of $a(\cdot,\cdot)$, and the last inequality follows from the finite element error bound (Lemma 7) and the interpolation error bound (Lemma 6 under $\|q\|_{H^{k+1}(\Omega)} \leq C\|\theta\|_{W^{k,4}(\Omega)}\|j_v\|_{W^{k-1,4}(\Omega)}$).

The procedure used to bound (V) is identical to (IV) with j_v and $\operatorname{div}\theta$ replaced by $\partial_x j_v$ and θ, respectively. We hence obtain $\text{(V)} \leq Ch^{2k}\|j_v\|_{W^{k,4}(\Omega)}\|\theta\|_{W^{k-1,4}(\Omega)}\|u\|_{H^{k+1}(\Omega)}$. The procedure used to bound (VI) and (VII) are identical to (IV) and (V), respectively, with j_v, $\partial_x j_v$, and u replaced by f, $\partial_x f$, and p, respectively.

We combine the bounds for (I)–(VII) to obtain the desired $\mathcal{O}(h^{2k})$ bound. □

4.3. Boundary-based shape derivative

We now present an *a priori* error analysis of the finite element approximation of the boundary-based shape derivative. Our analysis for the degree-k finite element approximation of linear elasticity problems again follows closely the analysis for the piecewise linear finite element approximation of Poisson's equation by Hiptmair et al. [16].

In order to provide a bound for the boundary-based shape derivative, we first make an additional assumption:

Assumption 5. *In the linear elasticity problem* (2)*, we assume that* Ω*,* f*,* g*,* j_v*, and* j_b *are sufficiently regular such that the finite element approximations of the solution* u *and the adjoint* p *satisfy, for any* $q \in (1,\infty]$*,*

$$\begin{aligned}
\|u-u_h\|_{W^{1,q}(\Omega)} &< Ch^k|u|_{W^{k+1,q}(\Omega)}, \\
\|p-p_h\|_{W^{1,q}(\Omega)} &< Ch^k|p|_{W^{k+1,q}(\Omega)},
\end{aligned}$$

where C *is a constant, independent of* u*,* p*, and* h*. Moreover, we assume that there exists a constant* $C' < \infty$ *such that* $\|u_h\|_{W^{1,q}(\Omega)} \leq C'\|u\|_{W^{1,q}(\Omega)}$ *and* $\|p_h\|_{W^{1,q}(\Omega)} \leq C'\|p\|_{W^{1,q}(\Omega)}$*.*

Remark 9. *Assumption 5 holds for sufficiently regular elliptic problems. See for example [10, Corollary 3.23].*

We now state the main result:

Theorem 10. *Let $u \in \mathcal{U}(\Omega)$ and $p \in \mathcal{U}(\Omega)$ be the solutions to* (1) *and* (5)*, respectively, and $u_h \in \mathcal{U}_h(\Omega)$ and $p_h \in \mathcal{U}_h(\Omega)$ be the associated finite element approximations defined in Assumption 2. Then under Assumptions 2–5,*

$$|dJ(\Omega;\theta) - dJ_h^{\mathrm{Bdry}}(\Omega;\theta)| \leq Ch^k \|\theta \cdot n\|_{L^\infty(\partial\Omega)},$$

where $dJ_h^{\mathrm{Bdry}}(\Omega;\cdot)$ is the finite element approximation of the boundary-based shape derivative (6)*, and C is a constant independent of h.*

Proof. We first appeal to the definition of the boundary-based shape derivative (6), invoke Hölder's inequality, and use the triangle inequality to split the error as

$$\begin{aligned}
&|dJ(\Omega;\theta) - dJ_h^{\mathrm{Bdry}}(\Omega;\theta)| \\
&\leq \left| \int_{\Gamma_{\mathrm{N}}} (j_v \cdot u - j_v \cdot u_h)\theta \cdot n \mathrm{d}s \right| + \left| \int_{\Gamma_{\mathrm{N}}} (-p \cdot f + p_h \cdot f)\theta \cdot n \mathrm{d}s \right| + \left| \int_{\Gamma_{\mathrm{N}}} (Ke(u) : e(p) - Ke(u_h) : e(p_h))\theta \cdot n \mathrm{d}s \right| \\
&\coloneqq (\mathrm{I}) + (\mathrm{II}) + (\mathrm{III}) \qquad (21)
\end{aligned}$$

We bound (I) by noting that

$$\begin{aligned}
(\mathrm{I}) &= \left| \int_{\Gamma_{\mathrm{N}}} (j_v \cdot (u - u_h))\theta \cdot n \mathrm{d}s \right| \leq \|\theta \cdot n\|_{L^\infty(\Gamma_N)} \|j_v\|_{L^1(\Gamma_N)} \|u - u_h\|_{L^\infty(\Gamma_N)} \\
&\leq Ch^k \|\theta \cdot n\|_{L^\infty(\Gamma_N)} \|j_v\|_{L^1(\Gamma_N)} |u|_{W^{k,\infty}(\Omega)},
\end{aligned}$$

where the first inequality follows from Hölder's inequality, and the second inequality follows from Assumption 5. The procedure to bound (II) is identical to (I) with j_v and u replaced by f and p, respectively.

A bound for (III) is given by

$$\begin{aligned}
(\mathrm{III}) &= \left| \int_{\Gamma_N} (Ke(u_h) : e(p - p_h) + Ke(p) : e(u - u_h))\theta \cdot n ds \right| \\
&\leq C\|\theta \cdot n\|_{L^\infty(\Gamma_N)} (\|u_h\|_{W^{1,1}(\Gamma_N)} \|p - p_h\|_{W^{1,\infty}(\Gamma_N)} + \|p\|_{W^{1,1}(\Gamma_N)} \|u - u_h\|_{W^{1,\infty}(\Gamma_N)}) \\
&\leq C'h^k \|\theta \cdot n\|_{L^\infty(\Gamma_N)} (\|u\|_{W^{1,1}(\Gamma_N)} |p|_{W^{k+1,\infty}(\Omega)} + \|p\|_{W^{1,1}(\Gamma_N)} |u|_{W^{k+1,\infty}(\Omega)}),
\end{aligned}$$

where the first inequality follows from Hölder's inequality, and the second inequality follows from Assumption 5. The combination of the bounds for (I)–(III) yields the desired $\mathcal{O}(h^k)$ error bound. □

Remark 11. *Recent work by Gong and Zhu [14] shows that, for scalar elliptic problems in a sufficiently regular domain, correction terms can be added to the boundary-based shape derivative to achieve $2k$-th order accuracy. However, the formulation requires domain regularity that may not be observed in practical linear elasticity optimization problems.*

4.4. Error analysis of the Riesz representation $\theta \in \mathcal{V}(\mathcal{D})$

Having analyzed the errors in the finite element approximation of the shape derivatives $dJ_h^{\text{Vol}}(\Omega;\cdot)$ and $dJ_h^{\text{Bdry}}(\Omega;\cdot)$, we now analyze the error in their Riesz representation $\theta^\star \in \mathcal{V}(\mathcal{D})$ given by (10). The finite element approximation of the Riesz representation is given by $\theta_h \in \mathcal{V}_h(\mathcal{D})$ such that

$$(\theta_h^\star, \xi_h)_{\mathcal{V}} = -dJ_h^{\text{Vol/Bdry}}(\Omega;\xi_h) \quad \forall \xi_h \in \mathcal{V}_h(\mathcal{D}), \tag{22}$$

where $\mathcal{V}_h(\mathcal{D})$ is the piecewise degree-k polynomial approximation of $\mathcal{V}(\mathcal{D})$. Our analysis for linear elasticity problems follows closely the analysis for piecewise linear finite element approximations of Poisson's equation by Paganini and Hiptmair [23].

The following lemma provides a decomposition of the error $\|\theta^\star - \theta_h^\star\|_{\mathcal{V}}$.

Lemma 12. *Let $\theta^\star \in \mathcal{V}(\mathcal{D})$ and $\theta_h^\star \in \mathcal{V}_h(\mathcal{D})$ be the solutions to* (10) *and* (22)*, respectively. Then*

$$\|\theta^\star - \theta_h^\star\|_{\mathcal{V}} \equiv 2 \inf_{\theta_h \in \mathcal{V}_h(\mathcal{D})} \|\theta^\star - \theta_h\|_{\mathcal{V}} + \sup_{\theta_h \in \mathcal{V}_h(\mathcal{D})} \frac{|dJ(\Omega;\theta_h) - dJ_h^{\text{Vol/Bdry}}(\Omega;\theta_h)|}{\|\theta_h\|_{\mathcal{V}}} \tag{23}$$

Proof. The result follows from Strang's first lemma [10, Lemma 2.27]. □

The first term of (23) is the best-fit error, which can be bounded using standard polynomial approximation theory. To bound the second term, we provide error bounds for dJ_h^{Vol} and dJ_h^{Bdry} when $\theta \in H^1(\Omega)^d$ (which is equivalent to $\mathcal{V}(\Omega)$) in the next two lemmas.

Lemma 13. *Let $u \in \mathcal{U}(\Omega)$ and $p \in \mathcal{U}(\Omega)$ be the solutions to* (1) *and* (5)*, respectively, and $u_h \in \mathcal{U}_h(\Omega)$ and $p_h \in \mathcal{U}_h(\Omega)$ be the associated finite element approximations defined in Assumption 2. Then under Assumptions 2–5 and assuming $\theta \in H^1(\Omega)^d$, $f \in W^{1,4}(\Omega)$, and $j_v \in W^{1,4}(\Omega)$,*

$$|dJ(\Omega;\theta) - dJ_h^{\text{Vol}}(\Omega;\theta)| \leq Ch^k \|\theta\|_{H^1(\Omega)}.$$

Proof. To begin, we decompose $|dJ(\Omega;\theta) - dJ_h^{\text{Vol}}(\Omega;\theta)|$ into terms (I)–(VII) identified in (19) in the proof of Theorem 8. We will bound the seven terms in order.

To bound (I), we note that

$$\begin{aligned}
\text{(I)} &\coloneqq \left| \int_\Omega (Du^T Ke(p) - Du_h^T Ke(p_h)) : D\theta \mathrm{d}x \right| \\
&= \left| \int_\Omega ((D(u-u_h))^T Ke(p) + Du_h^T Ke(p-p_h)) : D\theta \mathrm{d}x \right| \\
&\leq C(\|u-u_h\|_{W^{1,4}(\Omega)} \|p\|_{W^{1,4}(\Omega)} + \|u_h\|_{W^{1,4}(\Omega)} \|p-p_h\|_{W^{1,4}(\Omega)}) |\theta|_{H^1(\Omega)} \\
&\leq Ch^k (|u|_{W^{k+1,4}(\Omega)} \|p\|_{W^{1,4}(\Omega)} + \|u\|_{W^{1,4}(\Omega)} |p|_{W^{k+1,4}(\Omega)}) |\theta|_{H^1(\Omega)},
\end{aligned}$$

where the first inequality follows from Hölder's inequality, and the last inequality follows from Assumption 5. We use the same procedure to bound (II) and (III); we find both terms are bounded by the same expression.

To bound (IV), we note that

$$\begin{aligned}(\text{IV}) &:= \left|\int_\Omega (j_v \cdot (u-u_h))\text{div}(\theta)dx\right| \leq \|j_v\|_{L^4(\Omega)}\|u-u_h\|_{L^4(\Omega)}|\theta|_{H^1(\Omega)} \\ &\leq Ch^{k+1}\|j_v\|_{L^4(\Omega)}|u|_{W^{k+1,4}(\Omega)}|\theta|_{H^1(\Omega)},\end{aligned}$$

where the first inequality follows from Hölder's inequality, and the last inequality follows from Assumption 5. We bound (VI) using the same procedure, with f and p replacing j_v and u, respectively, to find (VI) $\leq Ch^{k+1}\|f\|_{L^4(\Omega)}|p|_{W^{k+1,4}(\Omega)}|\theta|_{H^1(\Omega)}$.

To bound (V), we note that

$$\begin{aligned}(\text{V}) &:= \left|\int_\Omega ((\partial_x j_v)\cdot(u-u_h))\cdot\theta dx\right| \leq |j_v|_{W^{1,4}(\Omega)}\|u-u_h\|_{L^4(\Omega)}\|\theta\|_{L^2(\Omega)} \\ &\leq Ch^{k+1}|j_v|_{W^{1,4}(\Omega)}|u|_{W^{k,4}(\Omega)}|\theta|_{H^1(\Omega)},\end{aligned}$$

where the first inequality follows from Hölder's inequality, and the last inequality follows from Assumption 5 and the Poincaré-Friedrichs inequality. We bound (VII) using the same procedure, with f and p replacing j_v and u, respectively, to find (VII) $\leq Ch^{k+1}|f|_{W^{1,4}(\Omega)}|p|_{W^{k,4}(\Omega)}|\theta|_{H^1(\Omega)}$. The combination of the bounds for (I)–(VII) yields the desired result. □

Lemma 14. *Let $u \in \mathcal{U}(\Omega)$ and $p \in \mathcal{U}(\Omega)$ be the solutions to (1) and (5), and $u_h \in \mathcal{U}_h(\Omega)$ and $p_h \in \mathcal{U}_h(\Omega)$ be the associated finite element approximations defined in Assumption 2. Then under Assumptions 2–5 and assuming $\theta \in H^1(\Omega)^d$, $f \in W^{1,4}(\Omega)$, and $j_v \in W^{1,4}(\Omega)$,*

$$|dJ(\Omega;\theta) - dJ_h^{\text{Bdry}}(\Omega;\theta)| \leq Ch^k\|\theta\|_{H^1(\Omega)}.$$

Proof. To begin, we decompose $|dJ(\Omega;\theta) - dJ_h^{\text{Bdry}}(\Omega;\theta)|$ into terms (I)–(III) identified in (21) in the proof of Theorem 10. We will bound the three terms in order.

To bound (I), we observe

$$\begin{aligned}(\text{I}) &= \left|\int_{\Gamma_N} (j_v\cdot(u-u_h))\theta\cdot n ds\right| \leq \|\theta\cdot n\|_{L^2(\Gamma_N)}\|j_v\|_{L^2(\Gamma_N)}\|u-u_h\|_{L^\infty(\Gamma_N)} \\ &\leq Ch^k\|\theta\|_{H^1(\Omega)}\|j_v\|_{L^2(\Gamma_N)}|u|_{W^{k,\infty}(\Omega)},\end{aligned}$$

where the first inequality follows from Hölder's inequality, and the second inequality follows from Assumption 5 and the trace inequality. We bound (II) using the same procedure with j_v and u replaced by f and p, respectively. To bound (III), we observe

$$\begin{aligned}(\text{III}) &= \left|\int_{\Gamma_N} (Ke(u_h):e(p-p_h) + Ke(p):e(u-u_h))\theta\cdot n ds\right| \\ &\leq C\|\theta\cdot n\|_{L^2(\Gamma_N)}(\|u_h\|_{W^{1,2}(\Gamma_N)}\|p-p_h\|_{W^{1,\infty}(\Gamma_N)} + \|p\|_{W^{1,2}(\Gamma_N)}\|u-u_h\|_{W^{1,\infty}(\Gamma_N)}) \\ &\leq C'h^k\|\theta\|_{H^1(\Omega)}(\|u\|_{W^{1,2}(\Gamma_N)}|p|_{W^{k+1,\infty}(\Omega)} + \|p\|_{W^{1,2}(\Gamma_N)}|u|_{W^{k+1,\infty}(\Omega)}),\end{aligned}$$

where the first inequality follows from Hölder's inequality, and the second inequality follows from Assumption 5 and the trace inequality. The combination of the bounds for (I)–(III) yields the desired bound. □

The combination of Lemmas 12, 13, and 14 yield the following error bound for $\theta_h^\star$.

Theorem 15. *Let $\theta^\star \in \mathcal{V}(\mathcal{D})$ and $\theta_h^\star \in \mathcal{V}_h(\mathcal{D})$ be the solutions to (10) and (22), respectively, for the volumetric shape derivative $dJ^{\mathrm{Vol}}(\cdot,\cdot)$. If $\theta \in H^{k+1}(\mathcal{D})$ and the assumptions of Lemma 13 hold, the error is bounded by*

$$\|\theta^\star - \theta_h^\star\|_{\mathcal{V}} \leq Ch^k.$$

The same result holds for the boundary-based shape derivative $dJ^{\mathrm{Bdry}}(\cdot,\cdot)$ if the assumptions of Lemma 14 hold.

Proof. We begin with Lemma 12,

$$\|\theta^\star - \theta_h^\star\|_{\mathcal{V}} \equiv 2 \inf_{\theta_h \in \mathcal{V}_h(\mathcal{D})} \|\theta^\star - \theta_h\|_{\mathcal{V}} + \sup_{\theta_h \in \mathcal{V}_h(\mathcal{D})} \frac{|dJ(\Omega;\theta_h) - dJ_h(\Omega;\theta_h)|}{\|\theta_h\|_{\mathcal{V}}} := (\mathrm{I}) + (\mathrm{II}).$$

The term (I) is bounded by

$$(\mathrm{I}) \leq C \inf_{\theta_h \in \mathcal{V}_h(\mathcal{D})} \|\theta^\star - \theta_h\|_{H^1(\Omega)} \leq C|\theta^\star|_{H^{k+1}(\Omega)},$$

where the first inequality follows from the equivalence of $\|\cdot\|_{\mathcal{V}}$ and $\|\cdot\|_{H^1(\Omega)}$, and the second inequality follows from the polynomial approximation result for $\theta^\star \in H^{k+1}(\Omega)$. To bound (II), we appeal to Lemmas 13 and 14 for $dJ_h^{\mathrm{Vol}}(\cdot;\cdot)$ and $J_h^{\mathrm{Bdry}}(\cdot;\cdot)$, respectively, to obtain (II) $\leq Ch^k$. □

Theorem 15 shows that the descent direction $\theta_h^\star$ associated with both the volumetric and boundary-based shape derivatives converge as h^k in the $\mathcal{V}$ norm. However, Zhu et al. [31] has shown that, for scalar eigenvalue problems, the $L^2(\Omega)$ norm of the error in the volumetric descent direction converges as h^{k+1}. We present an extension of the analysis in [31] to linear elasticity problems. To begin, we assume that the following L^q error estimates hold for the state and adjoint:

Assumption 6. *In the linear elasticity problem (2), we assume that Ω, f, g, j_v, and j_b are sufficiently regular such that the finite element approximations of the solution u and the adjoint p satisfy, for any $q \in (1,\infty]$,*

$$\|u - u_h\|_{L^q(\Omega)} < Ch^{k+1}|u|_{W^{k+1,q}(\Omega)},$$
$$\|p - p_h\|_{L^q(\Omega)} < Ch^{k+1}|p|_{W^{k+1,q}(\Omega)},$$

where C is a constant, independent of u, p, and h.

Remark 16. *Assumption 6 holds for sufficiently regular elliptic problems. See for example [10, Proposition 3.24].*

We next introduce the following lemma:

Lemma 17. *Let $u \in \mathcal{U}(\Omega)$ and $p \in \mathcal{U}(\Omega)$ be the solutions to (1) and (5), respectively, and $u_h \in \mathcal{U}_h(\Omega)$ and $p_h \in \mathcal{U}_h(\Omega)$ be the associated finite element approximations defined in Assumption 2. Then under Assumptions 2–6 and assuming $\theta \in H^2(\Omega)^d$, $f \in W^{1,4}(\Omega)$, and $j_v \in W^{1,4}(\Omega)$,*

$$|dJ(\Omega;\theta) - dJ_h(\Omega;\theta)| \leq Ch^{k+1}\|\theta\|_{H^2(\Omega)}.$$

Proof. The proof closely follows the proof of Lemma 13, under the additional assumption (Assumption 6). To begin, we split (I) in the proof of Lemma 13 into two terms:

$$\begin{aligned}(\mathrm{I}) &\coloneqq \left|\int_\Omega (Du^T Ke(p) - Du_h^T Ke(p_h)) : D\theta \mathrm{d}x\right| = \left|\int_\Omega ((D(u-u_h))^T Ke(p) + Du_h^T Ke(p-p_h)) : D\theta \mathrm{d}x\right| \\ &\leq \left|\int_\Omega ((D(u-u_h))^T Ke(p)) : D\theta \mathrm{d}x\right| + \left|\int_\Omega (Du_h^T Ke(p-p_h)) : D\theta \mathrm{d}x\right| \coloneqq (\mathrm{I.1}) + (\mathrm{I.2}).\end{aligned}$$

To bound (I.1), we observe

$$\begin{aligned}(\mathrm{I.1}) = \Bigg|&\int_{\partial\Omega} (u-u_h)^T K(e(p)) D(\theta\cdot n)\mathrm{d}s - \int_\Omega (u-u_h)_c (D_a(Ke(p))_{cb})(D\theta)_{ab}\mathrm{d}x \\ &- \int_\Omega (u-u_h)^T Ke(p) D(\mathrm{div}(\theta))\mathrm{d}x\Bigg| \\ \leq\ & C\|u-u_h\|_{L^\infty(\Omega)}(\|p\|_{H^1(\partial\Omega)} + \|p\|_{W^{2,2}(\Omega)})\|\theta\|_{H^2(\Omega)},\end{aligned}$$

where the first equality follows from integration by parts, and the inequality follows from the successive application of the Hölder's inequality and the application of the trace theorem to the boundary term. Note that we express the contraction of a third-order tensor using the index notation. We then invoke Assumption 6 to obtain

$$(\mathrm{I.1}) \leq Ch^{k+1}|u|_{W^{k+1,\infty}(\Omega)}(\|p\|_{H^1(\partial\Omega)} + \|p\|_{W^{2,2}(\Omega)})\|\theta\|_{H^2(\Omega)}.$$

We use an analogous procedure to bound (I.2) to obtain $(\mathrm{I}) \leq Ch^{k+1}\|\theta\|_{H^2(\Omega)}$.

We repeat the procedure for (II) and (III) in Lemma 13 to obtain $(\mathrm{II}) \leq Ch^{k+1}\|\theta\|_{H^2(\Omega)}$ and $(\mathrm{III}) \leq Ch^{k+1}\|\theta\|_{H^2(\Omega)}$. To bound (IV)–(VII) in Lemma 13 by Ch^{k+1}, we simply note that $|\theta|_{H^1(\Omega)} \leq \|\theta\|_{H^2(\Omega)}$. □

Theorem 18. *Under the assumptions of Theorem 15 and Lemma 17, the error in $\theta_h^\star \in \mathcal{V}_h(\mathcal{D})$ is bounded by*

$$\|\theta^\star - \theta_h^\star\|_{L^2} \leq Ch^{k+1}.$$

Proof. To begin, we introduce $\tilde{\theta} \in \mathcal{V}(\mathcal{D})$ such that

$$(\tilde{\theta}, \xi)_{\mathcal{V}} = -dJ_h(\Omega;\xi) \quad \forall \xi \in \mathcal{V}(\mathcal{D}).$$

We then invoke the triangle inequality to decompose the error as

$$\|\theta^\star - \theta_h^\star\|_{L^2(\mathcal{D})} \leq \|\theta^\star - \tilde{\theta}\|_{L^2(\mathcal{D})} + \|\tilde{\theta} - \theta_h^\star\|_{L^2(\mathcal{D})} \coloneqq \text{(I)} + \text{(II)}.$$

To bound (I), we appeal to the Aubin-Nitsche trick [3] and Lemma 17. To begin, we introduce $y \in \mathcal{V}(\mathcal{D})$ such that

$$(y, \xi)_{\mathcal{V}} = (\theta^\star - \tilde{\theta}, \xi)_{L^2(\mathcal{D})} \quad \forall \xi \in \mathcal{V}(\mathcal{D}).$$

We then observe that

$$\|\theta^\star - \tilde{\theta}\|_{L^2(\mathcal{D})}^2 = (y, \theta^\star - \tilde{\theta})_{\mathcal{V}} = |dJ(\Omega; y) - dJ_h(\Omega; y)| \leq Ch^{k+1}\|y\|_{H^2(\mathcal{D})},$$

where the first equality follows from the definition of y, the second equality follows from the definition of $\theta^\star$ and $\tilde{\theta}$, and the inequality follows from Lemma 17. We invoke the elliptic regularity estimate $\|y\|_{H^2(\mathcal{D})} \leq C\|\theta^\star - \tilde{\theta}\|_{L^2(\mathcal{D})}$ to obtain

$$\text{(I)} = \|\theta^\star - \tilde{\theta}\|_{L^2(\mathcal{D})} \leq Ch^{k+1},$$

which is the desired bound for (I).

To bound (II), we again appeal to the Aubin-Nitsche trick. To begin, we introduce $z \in \mathcal{V}(\mathcal{D})$ such that

$$(z, \xi)_{\mathcal{V}} = (\tilde{\theta} - \theta_h^\star, \xi)_{L^2(\mathcal{D})} \quad \forall \xi \in \mathcal{V}(\mathcal{D}).$$

We then observe

$$\|\tilde{\theta} - \theta_h^\star\|_{L^2(\mathcal{D})}^2 = (z, \tilde{\theta} - \theta_h^\star)_{\mathcal{V}} = (z - \mathcal{I}_h z, \tilde{\theta} - \theta_h^\star)_{\mathcal{V}} \leq \|z - \mathcal{I}_h z\|_{\mathcal{V}}\|\tilde{\theta} - \theta_h^\star\|_{\mathcal{V}} \leq Ch\|z\|_{H^2(\mathcal{D})}\|\tilde{\theta} - \theta_h^\star\|_{\mathcal{V}},$$

where the first equality follows from the definition of z, the second equality follows from Galerkin orthogonality, the third equality follows from Cauchy-Schwarz, and the inequality follows from the interpolation error bound. We again invoke elliptic regularity estimate $\|z\|_{H^2(\Omega)} \leq C\|\tilde{\theta} - \theta_h^\star\|_{L^2(\mathcal{D})}$ to obtain

$$\text{(II)} = \|\tilde{\theta} - \theta_h^\star\|_{L^2(\mathcal{D})} \leq Ch\|\tilde{\theta} - \theta_h^\star\|_{\mathcal{V}} \leq Ch\|\theta^\star - \theta_h^\star\|_{\mathcal{V}} + Ch\|\theta^\star - \tilde{\theta}\|_{\mathcal{V}} \coloneqq \text{(II.1)} + \text{(II.2)}.$$

To bound (II.1), we appeal to Theorem 15 to obtain $\|\theta^\star - \theta_h^\star\|_{\mathcal{V}} \leq Ch^k$. To bound (II.2), we note that

$$\|\theta^\star - \tilde{\theta}\|_{\mathcal{V}}^2 = (\theta^\star - \tilde{\theta}, \theta^\star - \tilde{\theta})_{\mathcal{V}} = |dJ(\Omega; \theta^\star - \tilde{\theta}) - dJ_h(\Omega; \theta^\star - \tilde{\theta})| \leq Ch^k\|\theta^\star - \tilde{\theta}\|_{H^1(\Omega)},$$

where the second equality follows from the definition of $\theta^\star$ and $\tilde{\theta}$, and the inequality follows from Lemma 13. Since $\|\cdot\|_{\mathcal{V}}$ and $\|\cdot\|_{H^1(\Omega)}$ are equivalent, $\|\theta^\star - \tilde{\theta}\|_{\mathcal{V}} \leq Ch^k$. We combine the bounds for (II.1) and (II.2) to obtain (II) $\leq Ch^{k+1}$, which is the desired result. □

Theorem 18 shows that, under suitable regularity assumptions, the descent direction associated with the volumetric shape derivative converges as h^{k+1} in the $L^2(\mathcal{D})$ norm. We are unable to obtain a similar result for the boundary-based derivative; we will numerically validate the lower convergence rate of the boundary-based shape derivative in Section 5.1.

4.5. Remarks

Theorems 8 and 10 provide *a priori* error estimates for the linear finite element approximation of the volumetric shape derivative (8) and boundary-based shape derivative (7), respectively. We first observe that, for a sufficiently regular problem, the volumetric shape derivative is $2k$-th order accurate, while the boundary-based shape derivative is only k-th order accurate. In practice, the higher-order accuracy of the volumetric shape derivative implies that a coarser finite element mesh may be used to provide a shape derivative of a similar quality, which leads to a reduction in the computational cost. We also note that the level-set representation and the linear ($k = 1$) finite element approximation used in typical topology optimization are both second-order accurate in $\|\cdot\|_{L^2(\Omega)}$, and hence the error in the linear finite element approximation of the volumetric shape derivative converges at the same rate as the level-set representation.

Lemma 12 shows the error in the shape gradient θ consists of two terms: the best-fit error and consistency error. The choice of the shape derivative affects the latter. Theorem 15 shows that, in terms of the asymptotic convergence rate in $\|\cdot\|_{\mathcal{V}}$ (which is equivalent to $\|\cdot\|_{H^1(\mathcal{D})}$), both the volumetric and boundary-based shape gradients are k-th order accurate. However, Lemma 18 shows that the volumetric shape gradient converges as h^{k+1} in $\|\cdot\|_{L^2(\mathcal{D})}$. A numerical example in Section 5.1 will confirm that the volumetric shape gradient converges more rapidly than the boundary-based shape gradient in $\|\cdot\|_{L^2(\mathcal{D})}$ for some problems.

Comparing the expressions for the volumetric shape derivative (8) and boundary-based shape derivatives (6), we also note that the former requires the finite element approximations u_h and p_h to be in $H^1(\Omega)$ whereas the latter requires the approximations to be in $H^2(\Omega)$. In addition to the finite element approximations of the solution fields, the boundary of the structure Ω only requires Lipschitz continuity for the volumetric shape derivative (8), whereas the boundary-based shape derivative (6) requires the boundary of Ω be $\mathcal{C}^2$ regular. These regularity requirements for the boundary-based shape derivatives are not strictly satisfied by the approximations based on linear finite elements and, as noted in [9, Chapter 1, Section 5], could "lead to serious computational errors."

5. Numerical results

5.1. Verification of shape derivative convergence rate

We first verify the convergence behavior predicted by Theorems 8 and 10 using two numerical examples. The first example assesses the convergence of various polynomial degree finite element approximations for idealized, smooth solutions. The second example assesses the convergence for less regular solutions, which typically arise in topology optimization.

For the first example, we generate a smooth solution using the method of manufactured solutions. We

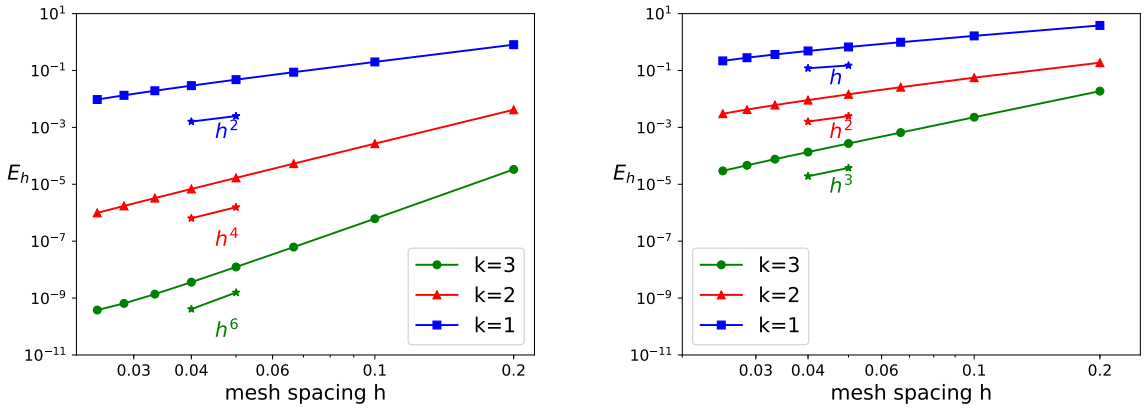

(a) volumetric derivative

(b) boundary-based derivative

Figure 1: Convergence of shape derivatives for $k = 1, 2, 3$ finite element approximations for the smooth manufactured problem.

consider the unit square domain $\Omega \equiv (0,1)^2$ and the manufactured solution

$$u_{\text{exact}}(x \equiv (x_1, x_2)) = \begin{bmatrix} e^{x_1 x_2} \sin(\pi x_1) \sin(\pi x_2) \\ 0 \end{bmatrix}, \tag{24}$$

which results from choosing $f = -\operatorname{div}(Ke(u_{\text{exact}}))$ and setting the homogeneous Dirichlet boundary conditions on all boundaries, i.e. $\Gamma_D = \partial\Omega$ and $\Gamma_N = \emptyset$. The compliance objective function is $J(\Omega) \coloneqq \int_\Omega f \cdot u \mathrm{d}x$.

As the evaluation of the true worst-case convergence rate of the shape derivative over all possible directions $\theta \in W^{1,\infty}(\Omega)^2$ is challenging, we follow the methods used by Hiptmair et al. [16] and restrict θ to the (vector-valued) cubic polynomial space $\mathbb{P}^3(\Omega)^2$. Specifically, we measure the convergence in the approximate dual norm

$$E_h^{\text{Vol/Bdry}} := \left(\max_{\theta \in \mathbb{P}^3(\Omega)^2} \frac{1}{\|\theta\|^2_{H^1(\Omega)}} \left| dJ(\Omega;\theta) - dJ_h^{\text{Vol/Bdry}}(\Omega;\theta) \right|^2 \right)^{1/2}. \tag{25}$$

The "true" value of $dJ(\Omega;\theta)$ is obtained on a sufficiently refined mesh. This error-evaluation problem can be cast as an eigenproblem through a Rayleigh-quotient-like interpretation [16]. Namely, we first introduce a basis $\{\theta_r\}_{r=1}^{m:=20}$ for the (vector-valued) cubic polynomial space $\mathbb{P}^3(\Omega)^2$. We then solve the eigenproblem $\mathbf{v}A\mathbf{v} = \lambda \mathbf{M}\mathbf{v}$, where $\mathbf{A} \coloneqq \mathbf{z}\mathbf{z}^T$ for a vector $\mathbf{z} = \left(dJ(\Omega;\theta_r) - dJ_h^{\text{Vol/Bdry}}(\Omega;\theta_r) \right)_{r=1}^m$, and $\mathbf{M} = ((\theta_i, \theta_j)_{H^1(\Omega)})_{i,j=1}^m$. The square root of the largest eigenvalue is the error given by the expression (25).

Figure 1 shows the error convergence behavior for the volumetric and boundary-based shape derivatives for this problem with smooth manufactured solution. We consider finite element polynomial degrees of $k = 1, 2, 3$. As predicted by Theorems 8 and 10, the errors in volumetric and boundary-shape derivatives are $\mathcal{O}(h^{2k})$ and $\mathcal{O}(h^k)$, respectively.

For the second example, we consider a cantilever beam problem, shown in Figure 2a; the cantilever is a unit square $\Omega \equiv (0,1)^2$. The beam is fixed on the left end, and is uniformly loaded on the right end over

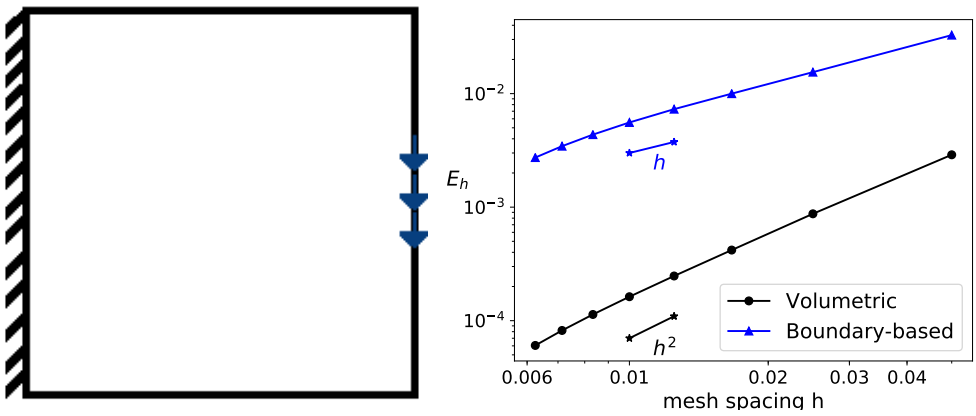

(a) cantilever beam configuration

(b) shape derivative convergence

Figure 2: Cantilever problem: problem description and convergence for linear finite element approximation.

the interval $(0.45, 0.55)$. We consider the compliance objective function $J(\Omega) := \int_{\partial\Omega} g \cdot u ds$. Compliance minimization of a cantilever beam subjected to traction loading is chosen as it is a standard test case within topology optimization literature.

Figure 2b shows the error convergence behavior for the volumetric and boundary-based shape derivatives for the cantilever problem using linear finite elements. The volumetric and boundary-based shape derivatives numerically observed convergence rates are in agreement with our theoretical analysis, stated in Theorems 8 and 10. In addition, the volumetric shape derivative is significantly more accurate than the boundary-based derivative even on a coarse mesh.

In addition to validating the convergence rates of the shape derivative θ, we also verify the effects of the extension and smoothing step on the descent direction, $\theta^\star$, predicted by Theorems 15 and 18. To demonstrate the convergence rates of the descent directions associated with the volumetric and boundary-based shape derivatives, we again consider the example problem with the manufactured solution (24). The convergence of the descent direction error is measured in the H^1 norm and L^2 norm: i.e., $\|\theta^\star - \theta_h^\star\|_{H^1(\Omega)}$ and $\|\theta^\star - \theta_h^\star\|_{L^2(\Omega)}$. The "true" value of $\theta^\star$ is obtained on a sufficiently refined mesh, for both the volumetric and boundary-based descent directions.

Figure 3 shows the H^1 error for the volumetric and boundary-based descent directions for this problem with a smooth manufactured solution. We consider finite element polynomial degrees of $k = 1, 2, 3$. The error in the smooth descent direction is $\mathcal{O}(h^k)$ in the H^1 norm, which is in agreement with Theorem 15. Similarly, Figure 4 shows the L^2 error for the volumetric and boundary-based descent directions. We observe that the L^2 error is $\mathcal{O}(h^{k+1})$ for the volumetric descent direction, which is consistent with Theorem 18. On the other hand, the L^2 error is $\mathcal{O}(h^k)$ for the boundary-based descent direction. Volumetric descent direction achieves higher convergence rates and is more accurate for the same mesh resolution in practice. It should

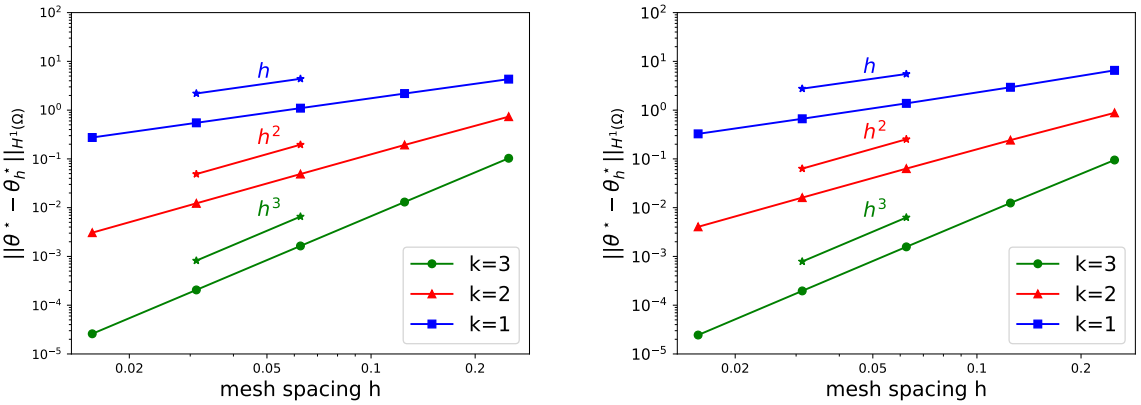

(a) Volumetric descent direction

(b) Boundary-based descent direction

Figure 3: Convergence of the H^1 error of the descent direction, $\theta^\star$, for $k = 1, 2, 3$ finite element approximations for the smooth manufactured problem.

be noted that the boundary-based and volumetric descent directions converge toward different values, due to the insufficient regularity of the domain Ω.

5.2. Topology optimization comparison

We now assess the practical impact of the choice of the shape derivative expressions on topology optimization. The volumetric shape derivative implementation uses the shape derivative (9), the descent direction extension (10), and the advection equation update step (11). The boundary-based shape derivative implementation uses the shape derivative (12), the descent direction extension (13), and the Hamilton-Jacobi equation update step (14). Our goal is to assess the robustness of the topology optimization procedure with respect to three different algorithm parameters that appear in Algorithm 1 described in Section 3.4:

1. *Descent direction extension.* We vary the behavior of the descent direction extension (10) and (13) by changing the parameter α from 10^{-2} to 10^2. A lower value of α results in a smoother extension, but may result in the loss of fine-scale features.
2. *Level-set evolution time step.* We vary the time step Δt used to evolve the level set function using (11) and (14) from 1 to 16 CFL unit. The design evolves more rapidly for a larger Δt, but may result in oscillatory convergence due to overshoot.
3. *Level-set reinitialization interval.* We consider algorithms with and without level set initialization by (15). As discussed in Section 3.4, the level-set loses the signed-distance property and may become too flat or steep without reinitialization.

We will refer to the numerical studies associated with the impact of the above three parameters as Case Study 1, 2, and 3, respectively. Ideally, the topology optimization algorithm should be robust with respect

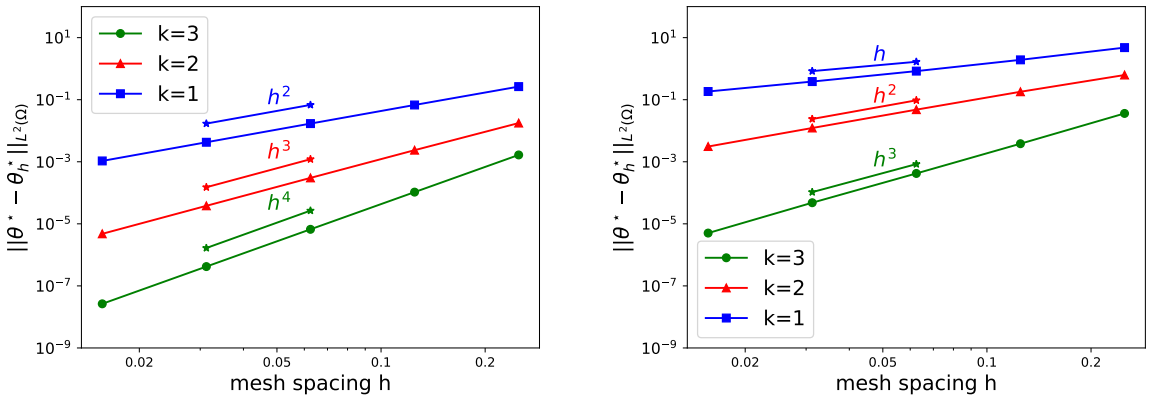

(a) Volumetric descent direction

(b) Boundary-based descent direction

Figure 4: Convergence of the L^2 error of the descent direction, $\theta^\star$, for $k = 1, 2, 3$ finite element approximations for the smooth manufactured problem.

to changes in these algorithm parameters that are often defined by the user in an ad-hoc manner.

All of the Case Studies are conducted using an implementation based on the FEniCS topology optimization code by Laurain [18]. A finite element approximation with linear elements is used for the linear elasticity equations, the shape derivative, and the descent direction. The default parameters are those implemented in the original FEniCS code: a smoothing parameter of $\alpha = 0.1$; the nominal evolution step time step of $\Delta t = 10$ CFL; and the level-set reinitialization interval of 5 iterations. The ersatz material method is used, with a ersatz material value of $\epsilon = 10^{-3}$. In Case Studies 1 and 3, we use a simple line search algorithm to adjust the nominal time step: in each level-set update step, the algorithm starts with the nominal Δt of 10 CFL, checks if the value of the objective function $J(\Omega)$ has decreased, and, if not, reduces the timestep by a factor of 0.8 until $J(\Omega)$ decreases (i.e., tries Δt, $0.8\Delta t$, $0.8^2\Delta t$, and $0.8^3\Delta t$). If the objective function $J(\Omega)$ does not decrease for the update associated with $0.8^3\Delta t$, it still accepts the update, reduces the nominal timestep by 0.8 for the next iteration, and continues with the optimization procedure. In Case Study 2, we use a fixed Δt without a line search.

Throughout this section, we consider a variant of the cantilever problem shown in Figures 2a extended to $\Omega \equiv (0, 2) \times (0, 1)$ with a volume-penalized compliance function

$$J(\Omega) = \int_\Omega g \cdot u \mathrm{d}x + \lambda V(\Omega) \tag{26}$$

for $\lambda = 50$. The finite element mesh contains 150×75 nodes. The initial design and final optimized design for the cantilever beam problem are shown in Figure 5; the volumetric and boundary-based shape derivatives yield visually indistinguishable structures.

Remark 19. *The boundary-based shape derivative implementation uses ersatz material and the "natural*

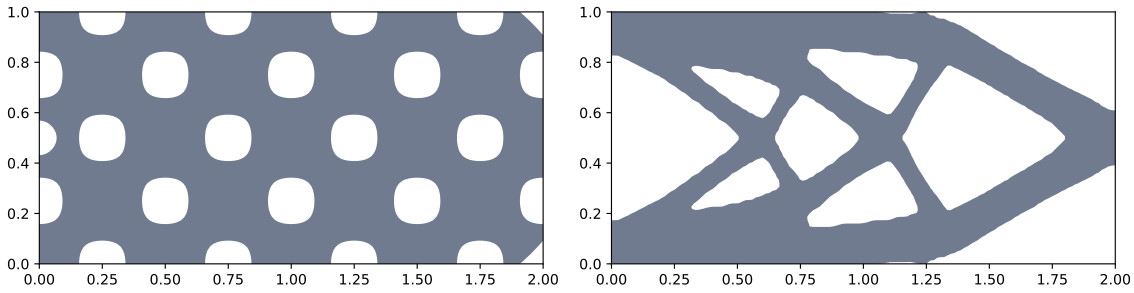

(a) Initial setup

(b) Optimized cantilever structure

Figure 5: Initial and final optimized structure for cantilever optimization problem.

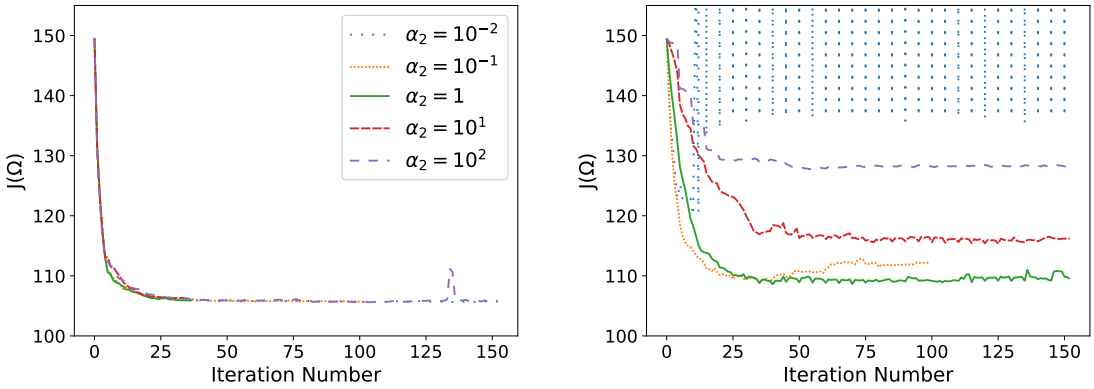

(a) Volumetric shape derivative

(b) Boundary-based shape derivative

Figure 6: Case Study 1: the effect of descent direction smoothing parameter α on topology optimization.

extension" descent direction (12). *As discussed in Section 3.5, these techniques introduce error in the numerical approximation of the solution u and the shape derivative dJ^{Bdry}; however, in practice, they provide (arguably favorable) smoothing of the descent direction when performing topology optimization.*

Case Study 1. We vary the behavior of the descent-direction extension (10) by changing α from 10^{-2} to 10^{2}. Figure 6 shows the result of the study. We observe that the algorithm based on the volumetric shape derivative is robust across a wide range of smoothing parameter values, producing similar results for each α. The boundary-based shape derivative is more sensitive to the choice of the smoothing parameter α, resulting in suboptimal results for all except $\alpha = 0.1$.

Case Study 2. We vary the fixed time step Δt used to evolve the level set function using (11) from 1 to 16 CFL unit. (Recall that, unlike the other case studies, we do not use line search in this case.) Figure 7 shows the result of the study. The algorithm based on the volumetric shape derivative converges to the same design, with exception of the $\Delta t = 16$ CFL case for which the solution oscillates around the optimal design. The main difference in the $\Delta t \in [1, 8]$ CFL cases is the rate of convergence to the optimal solution. The

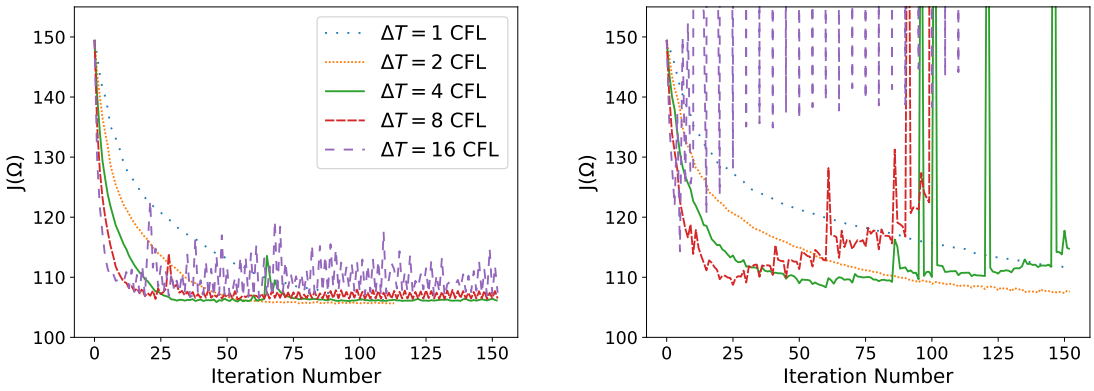

(a) Volumetric shape derivative

(b) Boundary-based shape derivative

Figure 7: Case Study 2: the effect of level-set evolution time step Δt on topology optimization.

cases with a higher Δt exhibit more rapid convergence in the beginning but is more prone to oscillations.

The algorithm based on the boundary-based shape derivative exhibits very different behaviors. For $\Delta t \in [1, 2]$ CFL, the objective function decreases steadily but takes many iterations to reach the optimal design; the $\Delta t = 1$ CFL is not fully converged even after 150 iterations. For a larger Δt, the algorithm fails to converge and the objective function oscillates significantly.

Case Study 3. We consider the optimization algorithm with and without level-set reinitialization using (15). Figure 8 shows the result of the study. We observe that the algorithm based on the volumetric shape derivatives converges to the same solution regardless of whether we reinitialize or not; however, the algorithm with reinitialization exhibits a more stable convergence behavior. On the other hand, the algorithm based on the boundary-based shape derivative does not converge without reinitialization; in fact the objective function starts to increase after 30 iterations.

In summary, Case Studies 1–3 show that algorithms based on the volumetric shape derivative are more robust than the boundary-based shape derivative, with less sensitivity to user defined optimization parameters, more often converging to optimal designs, and with faster convergence. Hence, the volumetric shape derivative exhibits not only theoretical advantages as discussed in Section 4 but also practical advantages in topology optimization.

6. Conclusion

In this work, we studied the theoretical and practical impact of using boundary-based shape derivative and volumetric shape derivative in level-set-based topology optimization of linear elasticity systems. The analyses in Section 4 show that, for sufficiently regular problems, degree-k polynomial finite element approximations of the boundary-based and volumetric shape derivatives converge as h^k and h^{2k}, respectively.

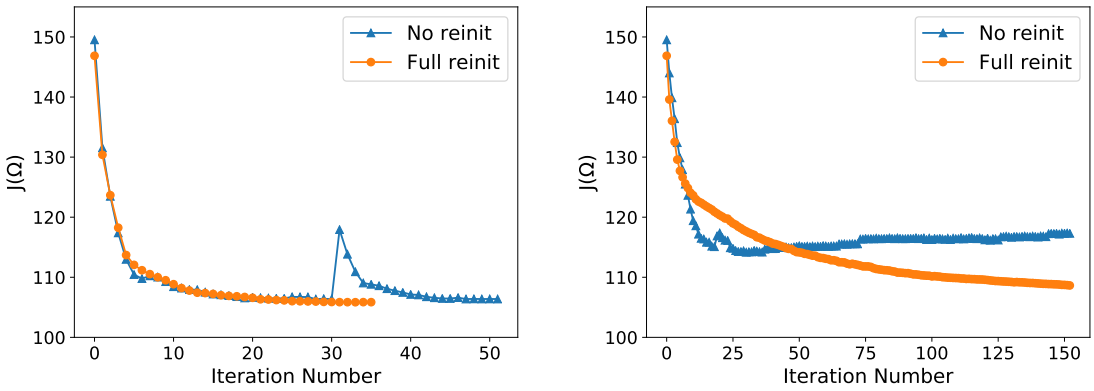

(a) Volumetric shape derivative

(b) Boundary-based shape derivative

Figure 8: Case Study 3: the effect of level-set reinitialization on topology optimization.

Moreover, the decent directions based on the boundary-based shape derivative converge as h^k in both H^1 and L^2 norms, whereas those based on the volumetric shape derivatives converge as h^k and h^{k+1} in the H^1 and L^2 norm, respectively. The numerical verification cases in Section 5 confirmed the predicted convergence rates of the shape derivatives and the descent directions. In a series of more practical numerical studies, topology optimization algorithms based on volumetric shape derivative exhibited faster convergence and less sensitivity to user-defined parameters. Both the theoretical analyses and numerical results suggest that, while currently not as widely used, volumetric shape derivative has the potential to significantly improve the efficiency and robustness of topology optimization algorithms, and it must be considered as a competitive alternative to boundary-based derivative.

Appendix A. Derivation of the boundary-based shape derivatives

We follow [1] to derive the boundary-based shape derivative for the first part of the linear objective functional (3) under the regularity assumptions stated in Section 3.2. To begin, we define the Lagrangian $\mathcal{L}(\Omega,\cdot,\cdot) : H^2(\Omega)^d \times H^2(\Omega)^d \to \mathbb{R}$ such that

$$\mathcal{L}(\Omega,v,q) \coloneqq \int_\Omega j_v \cdot v \mathrm{d}x + \int_{\Gamma_N} j_b \cdot v \mathrm{d}s + \int_\Omega Ke(v) : e(q) \mathrm{d}x - \int_\Omega q \cdot f \mathrm{d}s$$
$$- \int_{\Gamma_N} q \cdot g \mathrm{d}s - \int_{\Gamma_D} (q \cdot Ke(v)n + v \cdot Ke(q)n) \mathrm{d}s \quad \forall v,q \in H^2(\Omega)^d.$$

We next seek the stationary point of the Lagrangian: find $(u,p) \in H^2(\Omega)^d \times H^2(\Omega)^d$ such that

$$\begin{aligned}
\langle \partial_q \mathcal{L}(\Omega,u,p),\phi\rangle &= -\int_\Omega \phi\cdot(\mathrm{div}(Ke(u))+f)\mathrm{d}x + \int_{\Gamma_\mathrm{N}} \phi\cdot((Ke(u))n-g)\mathrm{d}s \\
&\quad -\int_{\Gamma_\mathrm{D}} u\cdot Ke(\phi)n\mathrm{d}s = 0 \quad \forall \phi\in H^2(\Omega)^d, \\
\langle \partial_v \mathcal{L}(\Omega,u,p),\phi\rangle &= \int_\Omega (j_v - \mathrm{div}(Ke(p)))\cdot\phi\mathrm{d}x + \int_{\Gamma_\mathrm{N}} \phi\cdot(Ke(p)n+j_b)\,\mathrm{d}s \\
&\quad -\int_{\Gamma_\mathrm{D}} p\cdot Ke(\phi)n\mathrm{d}s \quad \forall \phi\in H^2(\Omega)^d,
\end{aligned}$$

where $\langle\cdot,\cdot\rangle$ is the duality pairing in $H^2(\Omega)^d$, u is the solution to the linear elasticity problem (2) and p is the solution to the adjoint problem (5). Given the stationary point (u,p), the shape derivative is given by

$$\begin{aligned}
dJ(\Omega;\theta) &= \langle \partial_\Omega \mathcal{L}(\Omega,u,p),\theta\rangle \\
&= \int_{\partial\Omega} \theta\cdot n(j_v\cdot u + Ke(u):e(p) - p\cdot f)\mathrm{d}s \\
&\quad + \int_{\partial\Omega} \theta\cdot n\left(\frac{\partial(j_b\cdot u)}{\partial n} + Mj_b\cdot u\right)\mathrm{d}s \\
&\quad - \int_{\Gamma_\mathrm{N}} \theta\cdot n\left(\frac{\partial(g\cdot p)}{\partial n} + Mg\cdot p\right)\mathrm{d}s - \int_{\Gamma_\mathrm{D}} \theta\cdot n\left(\frac{\partial h}{\partial n} + Mh\right)\mathrm{d}s,
\end{aligned} \tag{A.1}$$

where $h \coloneqq u\cdot Ke(p)n + p\cdot Ke(u)n$. We recall that M is the curvature of $\partial\Omega$, which may be expressed as $M = \mathrm{div}\, n$ for $n = \nabla\phi/\|\nabla\phi\|$. We appeal to $u = p = 0$ on Γ_D to obtain (6).

Appendix B. Derivation of the volumetric shape derivatives

We derive the volumetric shape derivative expressions using the averaged adjoint method following [21, 18]. We first derive the volumetric shape derivative of the volume penalty $V(\Omega) \coloneqq \int_\Omega \mathrm{d}x$. We define the pseudo-time-parametrized volume and use change of variables to obtain

$$V(\Omega_t) \coloneqq \int_{\Omega_t} 1\mathrm{d}x = \int_\Omega \xi(t)\mathrm{d}x,$$

where $\xi(t) \coloneqq \det(D\Phi_t^\theta)$, and we recall that $\Omega_t = \Phi_t^\theta(\Omega)$. Since $\xi'(0) = \frac{d}{dt}\det(D\Phi_t^\theta)|_{t=0} = \mathrm{div}\ \theta$, the shape derivative simplifies to

$$dV^{\mathrm{Vol}}(\Omega;\theta) = \int_\Omega \mathrm{div}\,\theta\mathrm{d}x.$$

We next derive a volumetric shape derivative expression for the compliance functional. To this end, we first introduce the PDE-constrained optimization problem on the transformed domain Ω_t:

$$\begin{aligned}
&\min_{\Omega_t\subset\mathcal{D}} J(\Omega_t) = \int_{\Omega_t} j_v\cdot u_t\,\mathrm{d}x + \int_{\Gamma_{N,t}\equiv\Gamma_N} j_b\cdot u_t\mathrm{d}s + \lambda V(\Omega_t), \\
&\text{subject to} \quad \int_{\Omega_t} Ke(u_t):e(v)\mathrm{d}x = \int_{\Omega_t} f\cdot v\mathrm{d}x + \int_{\Gamma_{N,t}\equiv\Gamma_N} g\cdot v\mathrm{d}s \quad \forall v\in\mathcal{U}(\Omega_t),
\end{aligned} \tag{B.1}$$

where $u_t : \Omega_t \to \mathbb{R}^d$ is the solution in the transformed domain Ω_t. Note that we have $\Gamma_{N,t} \equiv \Gamma_N$ on the traction boundary and output boundary because by Assumption 1 these boundaries are fixed; i.e., $\Phi_t^\theta = I$ on Γ_N.

We now recast the problem on Ω. To this end, we introduce $u^t : \Omega \to \mathbb{R}^d$ given by $u^t \coloneqq u_t \circ \Phi_t^\theta$. The transformed problem is given by

$$\begin{aligned}
&\min_{\Omega_t \subset \mathcal{D}} J(\Omega_t) = \int_\Omega (j_v \circ \Phi_t^\theta) \cdot u^t \xi(t) \mathrm{d}x + \int_{\Gamma_N} j_b \cdot u^t \mathrm{d}s + \lambda V(\Omega_t), \\
&\text{subject to} \quad \int_\Omega KE(t,u^t) : E(t,v)\xi(t)\mathrm{d}x = \int_\Omega (f \circ \Phi_t^\theta) \cdot v \xi(t) \mathrm{d}x + \int_{\Gamma_N} g \cdot v ds \quad \forall v \in \mathcal{U}(\Omega_t),
\end{aligned}$$

where $E(t,u^t) \coloneqq e(u_t) \circ \Phi_t^\theta = ((Du^t)(D\Phi_t^\theta)^{-1} + (D\Phi_t^\theta)^{-T}(Du^t)^T)/2$ is the strain tensor in Ω_t expressed in Ω. We define the associated Lagrangian $G : [0,\tau] \times \mathcal{U}(\Omega) \times \mathcal{U}(\Omega) \to \mathbb{R}$ such that

$$\begin{aligned}
G(t,\varphi,\psi) \coloneqq &\int_\Omega (j_v \circ \Phi_t^\theta) \cdot \varphi \xi(t) \mathrm{d}x + \int_{\Gamma_N} j_b \cdot \varphi \mathrm{d}s + \int_\Omega KE(t,\varphi) : E(t,\psi)\xi(t)\mathrm{d}x \\
&- \int_\Omega (f \circ \Phi_t^\theta) \cdot \psi \xi(t) \mathrm{d}x - \int_{\Gamma_N} g \cdot \psi \mathrm{d}s \quad \forall \varphi, \psi \in \mathcal{U}(\Omega).
\end{aligned}$$

Since u^t by definition satisfies the linear elasticity equation recast on Ω, we have $J(\Omega_t) = G(t,u^t,\psi)$ for all $\psi \in H_d^1(\Omega)^d$. Hence the shape derivative may be expressed as

$$dJ(\Omega;\theta) = \frac{d}{dt}(G(t,u^t,\psi))|_{t=0} = \partial_t G(0,u^0,p^0), \tag{B.2}$$

where $p^0 \in \mathcal{U}(\Omega)$ is the adjoint

$$\langle \partial_\varphi G(0,u,p), \hat{\varphi} \rangle = \int_\Omega Ke(p^0) : e(\hat{\varphi}) \mathrm{d}x + \int_\Omega j_v \cdot \hat{\varphi} \mathrm{d}x + \int_{\Gamma_N} j_b \cdot \hat{\varphi} \mathrm{d}s = 0 \quad \forall \hat{\varphi} \in \mathcal{U}(\Omega);$$

note that the transformed equation at $t = 0$ simplifies because $\Phi_0 = I$, $E(0,v) = e(v)$, and $\xi(0) = 1$, and hence the equation is the same as the adjoint equation (5) introduced earlier. More explicitly (B.2) evaluates to

$$\begin{aligned}
dJ(\Omega;\theta) = &\int_\Omega (\partial j_v \cdot u) \cdot \theta \mathrm{d}x + \int_\Omega j_v \cdot u \operatorname{div}\theta \mathrm{d}x - \int_\Omega (\partial f \cdot p) \cdot \theta \mathrm{d}x - \int_\Omega f \cdot p \operatorname{div}\theta \mathrm{d}x \\
&+ \int_\Omega (K\partial_t E(0,u) : E(0,p) + KE(0,u) : \partial_t E(0,p)) \, \mathrm{d}x + \int_\Omega KE(0,u) : E(0,p) \operatorname{div}\theta \mathrm{d}x \\
= &-\frac{1}{2}\int_\Omega Du^T(Ke(p) + (Ke(p))^T) : D\theta \mathrm{d}x - \frac{1}{2}\int_\Omega Dp^T(Ke(u) + (Ke(u))^T) : D\theta \mathrm{d}x \\
&+ \int_\Omega Ke(u) : e(p) \operatorname{div}\theta \mathrm{d}x + \int_\Omega (\partial_x j_v \cdot u) \cdot \theta \mathrm{d}x + \int_\Omega j_v \cdot u \operatorname{div}\theta \mathrm{d}x \\
&- \int_\Omega (\partial_x f \cdot p) \cdot \theta \mathrm{d}x - \int_\Omega f \cdot p \operatorname{div}\theta \mathrm{d}x,
\end{aligned}$$

where the second equality follows from $\partial_t E(0,v) = (-(Dv)(D\theta) - (D\theta)^T(Dv)^T)/2$ and $E(0,v) = e(v)$, and we recall $\partial_x j_v$ and $\partial_x f$ are the spatial gradients of j_v and f, respectively. We finally appeal to the symmetry of K to obtain the volumetric shape derivative (8).

Acknowledgments

This work is supported by grants from the Natural Sciences and Engineering Research Council of Canada. We would also like to thank anonymous reviewers for very helpful feedback that has improved this manuscript.

References

[1] G. Allaire, F. Jouve, and A.-M. Toader. Structural optimization using sensitivity analysis and a level-set method. *Journal of Computational Physics*, 194(1):363–393, 2004.

[2] M. P. Bendsøe and N. Kikuchi. Generating optimal topologies in structural design using a homogenization method. *Computer Methods in Applied Mechanics and Engineering*, 71(2):197–224, 1988.

[3] S. C. Brenner and L. R. Scott. *The mathematical theory of finite element methods*. Springer, 1994.

[4] V. J. Challis. A discrete level-set topology optimization code written in MATLAB. *Structural and Multidisciplinary Optimization*, 41(3):453–464, 2010.

[5] M. Dambrine and D. Kateb. On the ersatz material approximation in level-set methods. *ESAIM: Control, Optimisation and Calculus of Variations*, 16(3):618–634, 2010.

[6] F. De Gournay. Velocity extension for the level-set method and multiple eigenvalues in shape optimization. *SIAM Journal on Control and Optimization*, 45(1):343–367, 2006.

[7] J. D. Deaton and R. V. Grandhi. A survey of structural and multidisciplinary continuum topology optimization: post 2000. *Structural and Multidisciplinary Optimization*, 49(1):1–38, 2014.

[8] M. Delfour, G. Payre, and J.-P. Zolésio. An optimal triangulation for second-order elliptic problems. *Computer Methods in Applied Mechanics and Engineering*, 50(3):231–261, 1985.

[9] M. C. Delfour and J.-P. Zolésio. *Shapes and geometries: metrics, analysis, differential calculus, and optimization*, volume 22 of *Adv. Design Control*. SIAM, 2011.

[10] A. Ern and J.-L. Guermond. *Theory and practice of finite elements*, volume 159. Springer Science & Business Media, 2013.

[11] T. Etling and R. Herzog. Optimum experimental design by shape optimization of specimens in linear elasticity. *SIAM Journal on Applied Mathematics*, 78(3):1553–1576, 2018.

[12] F. Feppon, G. Allaire, F. Bordeu, J. Cortial, and C. Dapogny. Shape optimization of a coupled thermal fluid–structure problem in a level set mesh evolution framework. *SeMA Journal*, 76(3):413–458, 2019.

[13] P. Gangl. Sensitivity-based topology and shape optimization with application to electric motors. In *Frontiers in PDE-Constrained Optimization*, pages 317–340. Springer, 2018.

[14] W. Gong and S. Zhu. On discrete shape gradients of boundary type for PDE-constrained shape optimization. *SIAM Journal on Numerical Analysis*, 59(3):1510–1541, 2021.

[15] J. Hadamard. *Mémoire sur le problème d'analyse relatif à l'équilibre des plaques élastiques encastrées*, volume 33. Imprimerie nationale, 1908.

[16] R. Hiptmair, A. Paganini, and S. Sargheini. Comparison of approximate shape gradients. *BIT Numerical Mathematics*, 55(2):459–485, Jun 2015.

[17] V. Komkov, K. K. Choi, and E. J. Haug. *Design Sensitivity Analysis of Structural Systems*. Elsevier Science & Techn., 1986.

[18] A. Laurain. A level set-based structural optimization code using FEniCS. *Structural and Multidisciplinary Optimization*, 58(3):1311–1334, 2018.

[19] A. Laurain. A level set-based structural optimization code using FEniCS. arXiv: 1705.01442, 2018.

[20] A. Laurain. Distributed and boundary expressions of first and second order shape derivatives in nonsmooth domains. *Journal de Mathématiques Pures et Appliquées*, 134:328–368, 2020.

[21] A. Laurain and K. Sturm. Distributed shape derivative via averaged adjoint method and applications. *ESAIM: Mathematical Modelling and Numerical Analysis*, 50(4):1241–1267, 2016.

[22] S. Osher and J. A. Sethian. Fronts propagating with curvature-dependent speed: algorithms based on Hamilton-Jacobi formulations. *Journal of Computational Physics*, 79(1):12–49, 1988.

[23] A. Paganini and R. Hiptmair. Approximate Riesz representatives of shape gradients. In L. Bociu, J. A. Desideri, and A. Habbal, editors, *System Modeling and Optimization. CSMO 2015. IFIP Advances in Information and Communication Technology, vol 494.*, pages 399–409. Springer, Cham., 2016.

[24] O. Sigmund and K. Maute. Topology optimization approaches. *Structural and Multidisciplinary Optimization*, 48(6):1031–1055, Dec 2013.

[25] K. Sturm. Minimax Lagrangian approach to the differentiability of nonlinear PDE constrained shape functions without saddle point assumption. *SIAM Journal on Control and Optimization*, 53(4):2017–2039, jan 2015.

[26] N. P. van Dijk, K. Maute, M. Langelaar, and F. Van Keulen. Level-set methods for structural topology optimization: a review. *Structural and Multidisciplinary Optimization*, 48(3):437–472, 2013.

[27] M. Y. Wang and P. Wang. The augmented Lagrangian method in structural shape and topology optimization with RBF based level set method. In *CJK-OSM 4: The Fourth China-Japan-Korea Joint Symposium on Optimization of Structural and Mechanical Systems*, page 191, 2006.

[28] M. Y. Wang, X. Wang, and D. Guo. A level set method for structural topology optimization. *Computer Methods in Applied Mechanics and Engineering*, 192(1-2):227–246, 2003.

[29] S. Zhu. Effective shape optimization of Laplace eigenvalue problems using domain expressions of Eulerian derivatives. *Journal of Optimization Theory and Applications*, 176(1):17–34, 2018.

[30] S. Zhu and Z. Gao. Convergence analysis of mixed finite element approximations to shape gradients in the Stokes equation. *Computer Methods in Applied Mechanics and Engineering*, 343:127–150, 2019.

[31] S. Zhu, X. Hu, and Q. Wu. On accuracy of approximate boundary and distributed h^1 shape gradient flows for eigenvalue optimization. *Journal of Computational and Applied Mathematics*, 365:112374, 2020.